Practical Stability Analysis of a Drilling Pipe Under Friction With a PI-Controller

Matthieu Barreau, Frédéric Gouaisbaut, and Alexandre Seuret

***Abstract*— This article deals with the stability analysis of a drilling pipe controlled by a PI controller. The model is a coupled ordinary differential equation/partial differential equation (PDE) and is consequently of infinite dimension. Using recent advances in time-delay systems, we derive a new Lyapunov functional based on a state extension made up of projections of the Riemann coordinates. First, we will provide an exponential stability result expressed using the linear matrix inequality (LMI) framework. This result is dedicated to a linear version of the torsional dynamic. On the other hand, the influence of the nonlinear friction force, which may generate the well-known stick-slip phenomenon, is analyzed through a new stability theorem. Numerical simulations show the effectiveness of the method and that the stick-slip oscillations cannot be weakened using a PI controller.**

***Index Terms*— Friction, linear matrix inequality (LMI), Lyapunov methods, oil drilling, partial differential equations (PDEs), PI control, stability analysis.**

I. Introduction

STUDYING the behavior of complex machineries is a real challenge since they usually present nonlinear and coupled behaviors [49]. A drilling mechanism is a very good example of this. Many nonlinear effects can occur on the drilling pipe, such as bit bouncing, stick-slip, or whirling [14]. These phenomena induce generally some vibrations, increasing the drill pipe fatigue and affecting, therefore, the life expectancy of the well. The first challenge is then to provide a dynamical model which reflects such behaviors.

Looking at the literature, many models exist from the simplest finite-dimensional ones presented in, for instance [13], [41], to the more complex but more realistic infinite-dimensional systems. Finite-dimensional systems were an important first step since they showed which characteristics are responsible for vibrations in the well. Nevertheless, they are too far from the physical laws which are expressed in terms of partial differential equation (PDE). Then, a coupled finite-/infinite-dimensional model seems more natural in the context of a drilling pipe, and it was proposed in [14], [20], and [38] for instance.

Manuscript received April 3, 2019; revised July 31, 2019; accepted September 16, 2019. Date of publication December 20, 2019; date of current version February 9, 2021. Manuscript received in final form September 19, 2019. This work was supported by the ANR project SCIDiS under Contract 15-CE23-0014. Recommended by Associate Editor Y. Orlov. *(Corresponding author: Matthieu Barreau.)*

The authors are with the Laboratory for Analysis and Architecture of Systems, Centre national de la recherche scientifique, Paul Sabatier University, 31062 Toulouse, France (e-mail: mbarreau@laas.fr; aseuret@laas.fr; fgouaisb@laas.fr).

Color versions of one or more of the figures in this article are available online at https://ieeexplore.ieee.org.

Digital Object Identifier 10.1109/TCST.2019.2943458

The second challenge was then to design a controller to remove, or at least weaken, these undesirable effects. Many control techniques were applied on the finite-dimensional model from the simple PI controller investigated in [13] and [15], to more advance controllers as sliding mode control [30] or H_∞ [41]. Nevertheless, extending these controllers on the coupled finite-/infinite-dimensional system is not straightforward.

The last decade has seen many developments regarding the analysis of infinite-dimensional systems. The semigroup theory, investigated in [48] for instance, was a great tool to simplify the proof of existence and uniqueness of a solution to this kind of problems. This leads to an extension of the Lyapunov theory to some classes of PDEs [9], [16], [33]. These advances have given rise to the stability analysis of the linearized infinite-dimensional drilling pipe with a PI controller [44], [45]. Since this kind of controller provides only two degrees of freedom, to better enhance the performances, slightly different controllers arose. One of the most famous is the modified PI controller in [47], but there is also a delayed PI or a flatness-based control in [38]. More complex controllers, coming from the backstepping technique for PDE, originally developed in [25], were also applied in [10], [12], and [35] for instance.

Nevertheless, these techniques almost always use a Lyapunov argument to conclude, and they consequently suffer from the lack of an efficient Lyapunov functional for coupled systems. Recent advances in the domain of time-delay systems [42] have lead to a hierarchy of Lyapunov functionals which are very efficient for coupled ordinary differential equation (ODE)/string equation [8]. Since it relies on a state extension, the stability analysis cannot be assessed manually, but it translates into an optimization problem expressed using linear matrix inequalities (LMIs) and consequently easily solvable.

This article takes advantage of this enriched Lyapunov functional to revisit the stability analysis of a PI-controlled infinite-dimensional model of a drilling pipe for the torsion only. The first contribution of this article results in Theorem 1, which provides an LMI to ensure the asymptotic stability of the linear closed-loop system. The second theorem deals with the practical stability of the controlled nonlinear plant. It shows, for example, that if the linear system is stable, the nonlinear system is also stable. Moreover, it provides an accurate bound on the oscillations during the stick-slip.

This article is organized as follows. Section II discusses the different models presented in the literature and enlighten the importance of treating the infinite-dimensional problem.

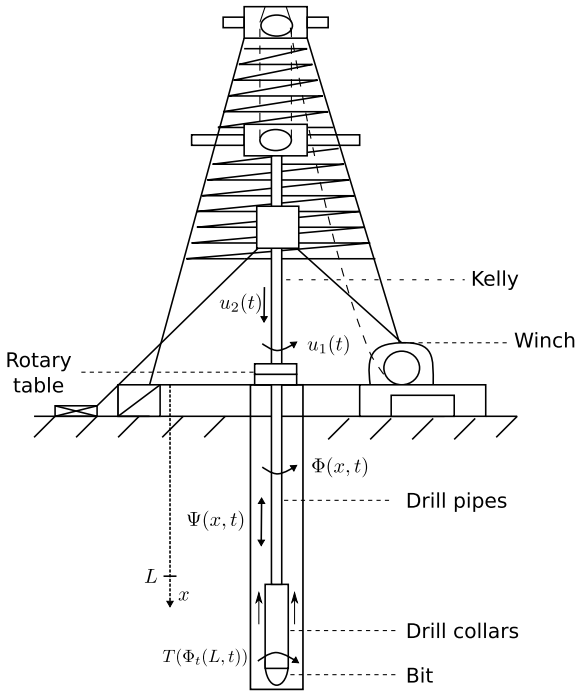

Fig. 1. Schematic of a drilling mechanism originally taken from [39]. Data corresponding to physical values are given in Table II.

Section III is the problem statement. Section IV is dedicated to the study of the linear system. This is a first step before dealing with the nonlinear system, which is the purpose of Section V. Finally, Section VI proposes simulations to demonstrate the effectiveness of this approach and conclude about the design of a PI controller.

Notations: For a multivariable function $(x,t) \mapsto u(x,t)$, the notation u_t stands for $(\partial u/\partial t)$ and $u_x = (\partial u/\partial x)$. We also use the notations $L^2 = L^2((0,1);\mathbb{R})$ and for the Sobolov spaces, $H^n = \{z \in L^2; \forall m \leqslant n, (\partial^m z/\partial x^m) \in L^2\}$. The norm in L^2 is $\|z\|^2 = \int_\Omega |z(x)|^2 dx =< z,z >$. For any square matrices A and B, the following operations are defined: $\mathrm{He}(A) = A + A^\top$ and $\mathrm{diag}(A,B) = \left[\begin{smallmatrix} A & 0 \\ 0 & B \end{smallmatrix}\right]$. The set of positive definite matrices of size n is denoted by $\mathbb{S}^n_+$ and, for simplicity, a matrix P belongs to this set if $P \succ 0$.

II. Model Description

A drilling pipe is a mechanism used to pump oil deep under the surface thanks to a drilling pipe, as shown in Fig. 1. Throughout the article, $\Phi(\cdot,t)$ is the twisting angle along the pipe, and then, $\Phi(0,t)$ and $\Phi(L,t)$ are the angles at the top and at the bottom of the well, respectively. The well is a long-metal rod of around one kilometer and consequently, the rotational velocity applied at the top using the torque $u_1(t)$ is different from the one at the bottom. Moreover, the interaction of the bit with the rock at the bottom is modeled by torque T, which depends on $\Phi_t(L,t)$.

As the bit drills the rock, axial compression of the rod occurs and is denoted Ψ. This compression arises because of the propagation along the rod of the vertical force u_2 applied at the top to push up and down the well.

This description leads naturally to two control objectives to prevent the mechanism from breaking. The first one is to maintain the rotational speed at the end of the pipe $\Phi(L,t)$ at a constant value, denoted here Ω_0, preventing any twisting of the pipe. The other one is to keep the penetration rate constant such that there is no compression along the rod.

Several models have been proposed in the literature to achieve these control objectives. They are of very different natures and lead to a large variety of analysis and control techniques. The book [38, Ch. 2] and the survey [40] provide overviews of these techniques, which are, basically, of four kinds. To better motivate the model used in the sequel, a brief overview of the existing modeling tools is proposed; but the reader can refer to [40] and the original articles to get a better understanding of how the models are constructed.

A. Lumped Parameter Models

These models are the first obtained in the literature [13], [27], [41] and the full mechanism is described by a sequence of harmonic oscillators. They can be classified into two main categories as follows.

1) The first kind assumes that the dynamics of the twisting angles $\Phi(0,t) = \Phi_r(t)$ (at the top) and $\Phi(L,t) = \Phi_b(t)$ (at the bottom) are described by two coupled harmonic oscillators. The torque u_1 driving the system is applied on the dynamic of Φ_r and the controlled angle is Φ_b. The axial dynamic is not taken into account in this model. This model can be found in [13], [32], and [41], for instance.
2) The other two degrees of freedom model is described in [27] and [34] for example. There also are two coupled harmonic oscillators for $\Psi(L,t)$ and $\Phi(L,t)$ representing the axial and torsional dynamics, respectively. This model only considers the motions at the end of the pipe and forget about the physics occurring along the rod.

The first class of models can be described by the following set of equations:

$$\begin{cases} I_r\ddot{\Phi}_r + \lambda_r(\dot{\Phi}_r - \dot{\Phi}_b) + k(\Phi_r - \Phi_b) + d_r\dot{\Phi}_r = u_1 \\ I_b\ddot{\Phi}_b + \lambda_b(\dot{\Phi}_b - \dot{\Phi}_r) + k(\Phi_b - \Phi_r) + d_b\dot{\Phi}_b = -T(\dot{\Phi}_b) \end{cases} \tag{1}$$

where the parameters are given in Table I. T is a torque modeled by a nonlinear function of $\dot{\Phi}_b$, and it describes the bit-rock interaction[1]. A second-order LPM can be derived by only taking into account the two dominant poles of the previous model.

An example of on-field measurements, shown in Fig. 2, shows the effect of this torque T on the angular speed. The periodic scheme which arises is called *stick-slip*. It emerges because of the difference between the static and Coulomb friction coefficients making an antidamping on the torque function T. Even though the surface angular velocity seems not to vary much, there is a cycle for the downhole one, and the angular speed is periodically close to zero, meaning that the bit is stuck to the rock.

The stick-slip effect appears mostly when dealing with a low-desired angular velocity Ω_0 on a controlled drilling mechanism. Indeed, if the angular speed $\Phi_t(L,t)$ is small,

[1] See [38, Ch. 3] for a detailed description about various models for T.

TABLE I
PARAMETERS VALUES AND THEIR MEANINGS FOR THE LPM TAKEN FROM [13], [32], AND [41]

Parameter meaning		Value
I_r	Rotary table and drive inertia	2122 kg.m^2
I_b	Bit and drillstring inertia	374 kg.m^2
k	Drillstring stiffness	1111 N.m.rad^{-1}
λ_r	Coupled damping at top	425 N.m.s.rad^{-1}
λ_b	Coupled damping at bottom	23.2 N.m.s.rad^{-1}
d_r	Rotary table damping	425 N.m.s.rad^{-1}
d_b	Bit damping	50 N.m.s.rad^{-1}
γ_b	Velocity decrease rate	0.9 s.rad^{-1}
μ_{cb}	Coulomb friction coefficient	0.5
μ_{sb}	Static friction coefficient	0.8
c_b	Bottom damping constant	0.03 N.m.s.rad^{-1}
T_{sb}	Static / Friction torque	15 145 N.m

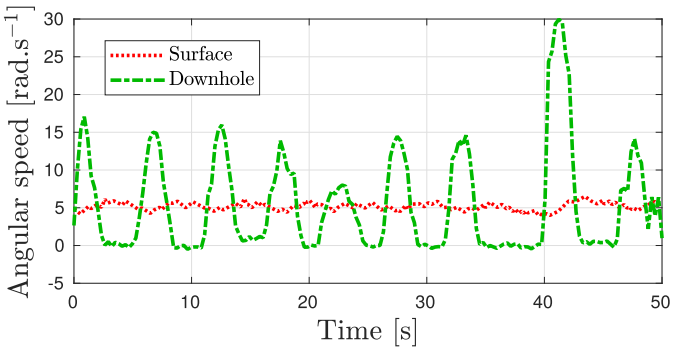

Fig. 2. Nonlinear effect on the drilling mechanism due to the friction torque at the bottom of the pipe. These measurements are done on the field [41].

the torque provided by the rotary table at $x = 0$ increases the torsion along the pipe. This increase leads to a higher $\Phi_t(L,t)$ but the negative damping on the torque function implies a smaller T. Consequently, $\Phi_t(L,t)$ increases, and this phenomenon is called the *slipping* phase. Then, the control law reduces the torque in order to match $\Phi_t(L,t)$ to Ω_0. Since the torque increases as well, that leads to a *sticking* phase where $\Phi(L,t)$ remains close to 0. A stick-slip cycle then emerges. Notice that this is not the case for high values of Ω_0 since torque T does not vary much with respect to $\Phi_t(L,t)$ making the system easier to control. In Fig. 2, one can see that the frequency of the oscillations is 0.17 Hz and its amplitude is between 10 and 25 rad.s^{-1}.

Modeling this phenomenon is of great importance as friction effects are quite common when studying mechanical machinery. Saldivar *et al.* [40] compare some models for T and conclude that they produce very similar results. The main characteristic is a decrease of T as $\Phi_t(L,t)$ increases. One standard model refers to the preliminary work of Karnopp [23]

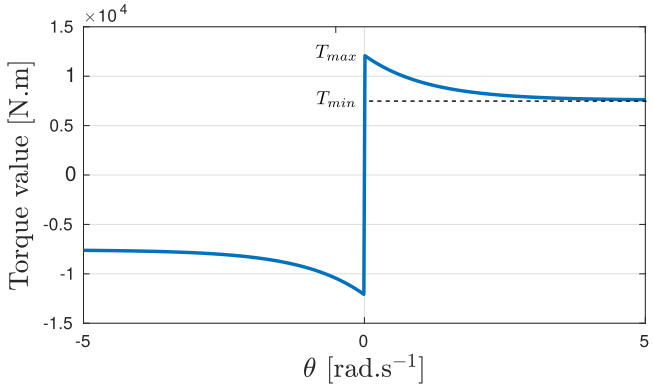

Fig. 3. Nonlinear part of the torque. T_{nl} is an approximation of the real friction torque coming from Karnopp [23].

and Armstrong-Helouvry *et al.* [3], [4] with an exponential decaying friction term, described in [31] for instance. This law (depicted in Fig. 3) is written thereafter where $\theta = \Phi_t(L,\cdot)$ is expressed in rad.s^{-1}

$$\begin{aligned} T(\theta) &= T_l(\theta) + T_{nl}(\theta) \\ T_l(\theta) &= c_b\theta \\ T_{nl}(\theta) &= T_{sb}(\mu_{cb} + (\mu_{sb} - \mu_{cb})e^{-\gamma_b|\theta|})\,\mathrm{sign}(\theta). \end{aligned} \tag{2}$$

This model has been used in [32] and [38], for instance.

Notice that an on-field description of this mechanism applied in the particular context of drilling systems is provided in [2] and concludes that these models are fair approximations of the nonlinear phenomena visible in similar structures.

At this stage, a lumped parameter model (LPM) is interesting for its simplicity but does not take into account the infinite-dimensional nature of the problem and, as a consequence, is a good approximation in the case of small vibrations only [39]. A deeper modeling can be done considering continuum mechanics and leading to a distributed parameter system.

B. Distributed Parameter Models (DPM)

To tackle the finite-dimensional approximation of the previous model, another one derived from mechanical equations leads to a set of PDEs as described in the works [14] and [49]. This model has been enriched in [1] and [2], where the system is presented from a control viewpoint and compared with on-field measurements. In the first articles, the model focuses on the propagation of the torsion only along the pipe. The axial propagation was introduced in the model by [1] and [40]. The new model is made up of two 1D wave equations representing each deformation for $x \in (0, L)$ and $t > 0$

$$\Phi_{tt}(x,t) = c_t^2\Phi_{xx}(x,t) - \gamma_t\Phi_t(x,t) \tag{3a}$$
$$\Psi_{tt}(x,t) = c_a^2\Psi_{xx}(x,t) - \gamma_a\Psi_t(x,t) \tag{3b}$$

where again Φ is the twist angle, Ψ is the axial movement, $c_t = (G/\rho)^{1/2}$ is the propagation speed of the angle, γ_t is the internal damping, $c_a = (E/\rho)^{1/2}$ is the axial velocity, and γ_a is the axial distributed damping. A list of physical parameters and their values is given in Table II, and Fig. 1

TABLE II
PHYSICAL PARAMETERS, MEANINGS, AND THEIR VALUES [1], [40]

Parameter meaning		Value
L	Pipe length	2000m
G	Shear modulus	79.3×10^9 N.m^{-2}
E	Young modulus	200×10^9 N.m^{-2}
Γ	Drillstring's cross-section	35×10^{-4} m^4
J	Second moment of inertia	1.19×10^{-5} m^4
I_B	Bottom hole lumped inertia	89 kg.m^2
M_B	Bottom hole mass	40 000 kg
ρ	Density	8000 kg.m^{-3}
g	Angular momentum	2000 N.m.s.rad^{-1}
h	Viscous friction coefficient	200 kg.s^{-1}
γ_a	Distributed axial damping	0.69 s^{-1}
γ_t	Distributed angle damping	0.27 s^{-1}
δ	Weight on bit coefficient	1 m^{-1}

helps giving a better understanding of the physical system. In other words, if $\Psi(\cdot, t) = 0$, then there is no compression in the pipe, meaning that the bit is not bouncing; if $\Phi_{tt}(\cdot, t) = 0$, then the angular speed along the pipe is the same, meaning that there is no increase or decrease of the torsion.

For the previous model to be well-posed, top and bottom boundary conditions (at $x = 0$ and $x = L$) must be incorporated in (3). In this part, only the topside boundary condition is derived. There is viscous damping at $x = 0$, and consequently a mismatch between the applied torque at the top and the angular speed. The topside boundary condition for the axial part is built on the same scheme, and the following conditions are obtained for $t > 0$:

$$GJ\Phi_x(0,t) = g\Phi_t(0,t) - u_1(t) \tag{4a}$$
$$E\Gamma\Psi_x(0,t) = h\Psi_t(0,t) - u_2(t). \tag{4b}$$

The downside boundary condition ($x = L$) is more difficult to grasp and is consequently derived later when dealing with a more complex model.

C. Neutral-Type Time-Delay Model

Studying an infinite-dimensional problem stated in terms of PDEs represents a relevant challenge. The equations obtained previously are damped wave equations, but for the special case where $\gamma_a = \gamma_t = 0$, the system can be converted into a neutral time-delay system as done in [38]. This new formulation enables to use other tools to analyze its stability as the Lyapunov–Krasovskii Theorem or a frequency-domain approach making its stability analysis slightly easier.

Nevertheless, the main drawback of this formulation is the assumption that the damping occurs at the boundary and not all along the pipe. This useful simplification, even if it encountered in many articles [12], [38], [39], is known to change in a significant manner the behavior of the system [1]. Indeed, it appears that without internal damping, the wave equation rephrases easily as a system of transport equations. It is then directly possible to observe with a delay of c^{-1} at the top of the pipe what happened at the bottom of the pipe. This makes control easier.

D. Coupled ODE/PDE Model

To overcome the issue mentioned earlier, a simpler model than the one derived in (3a) is proposed in [39], where a harmonic oscillator is used to describe axial vibrations and the model results in a coupled ODE/PDE.

A second possibility, reported in [14] and [38] for example, is to propose a second-order ODE as the bottom boundary condition ($x = L$) for $t > 0$

$$GJ\Phi_x(L,t) = -I_B\Phi_{tt}(L,t) - T(\Phi_t(L,t)) \tag{5a}$$
$$E\Gamma\Psi_x(L,t) = -M_B\Psi_{tt}(L,t) - \delta T(\Phi_t(L,t)) \tag{5b}$$

where T represents the torque applied on the drilling bit by the rocks, described in (2). Notice that (5a) is coming from the conservation of angular momentum, where $GJ\Phi_x(L,t)$ is the torque coming from the top of the pipe. Equation (5b) is the direct application of Newton's second law of motion, where $E\Gamma\Psi_x(L,t)$ is the force transmitted from the top to the bit and $\delta T(\Phi_t(L,t))$ is the weight on bit due to the rock interaction. Since (5a) is a second order in time differential equation, note that (3a) together with (5a) indeed leads to a coupled ODE/PDE.

There exist other bottom boundary conditions leading to more complex coupling between axial and torsional dynamics. They, nevertheless, introduce delays which require to have a better knowledge of the drilling bit. To keep the content general, the boundary conditions (5a) used throughout this article is proposed accordingly with [14], [39], and [45].

As a final remark, using some transformations based on (3a)–(5a), it is possible to derive a system for which backstepping controllers can be used [12], [37]. This is the main reason why this model is widely used today.

E. Models Comparison

We propose in this section to compare the coupled ODE/PDE model and the LPMs for the torsion only. We consider here a linearization of the system for large Ω_0, and consequently, we neglect the stick-slip effect by setting $T = 0$.

First, denote by $\mathcal{H}_{DPM}$ the transfer function from u_1 to $\Phi(L, \cdot)$ for the distributed parameter model (DPM) and $\mathcal{H}_{LPM}$ from u_1 to Φ_b for the LPM. We also define by $\mathcal{H}_{LPM2}$ a truncation of $\mathcal{H}_{LPM}$ considering only the two dominant poles. The Bode diagrams of $\mathcal{H}_{DPM}$, $\mathcal{H}_{LPM}$, and $\mathcal{H}_{LPM2}$ are drawn in Fig. 4.

Clearly, the LPMs catch the behavior of the DPM at steady states and low frequencies until the resonance occurring around $(k/I_b)^{1/2}$ rad.s^{-1}. From a control viewpoint, the DPM has infinitely many harmonics as it can be seen on the plots but

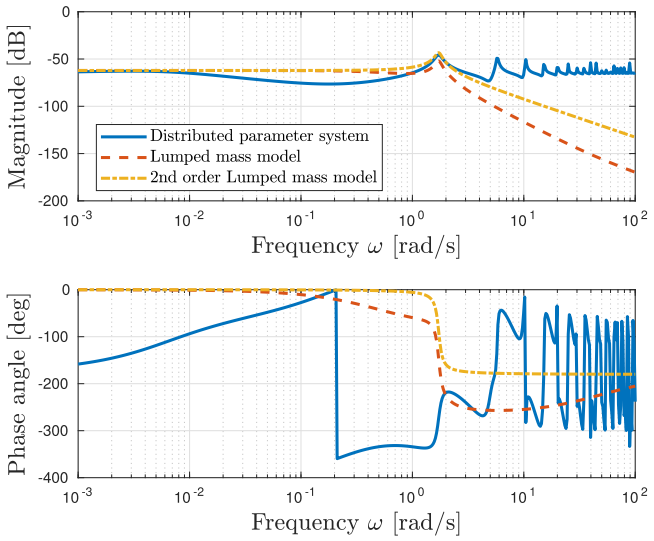

Fig. 4. Bode diagram of $\mathcal{H}_{DPM}$, $\mathcal{H}_{LPM}$, and $\mathcal{H}_{LPM2}$.

of lower magnitudes and damped as the frequency increases (around -10 dB at each decade). The magnitude plots are not sufficient to make a huge difference between the three models. Nevertheless, considering the phase, we see a clear difference. It appears that the DPM crosses the frequency -180 many times, making the control margins quite difficult to assess. Moreover, it shows that the DPM is harder to control because of the huge difference of behavior after the resonance. They may consequently have very different behavior when controlled. That is why we focus in this article on the DPM, even if it is far more challenging to control than the LPMs.

III. Problem Statement

The coupled nonlinear ODE/PDE model derived in Section II-B can be written as follows for $t > 0$ and $x \in [0, 1]$:

$$\begin{cases} \phi_{tt}(x,t) = \tilde{c}_t^2 \phi_{xx}(x,t) - \gamma_t \phi_t(x,t) \\ \phi_x(0,t) = \tilde{g}\phi_t(0,t) - \tilde{u}_1(t) \\ \phi_t(1,t) = z_1(t) \\ \dot{z}_1(t) = -\alpha_1 \phi_x(1,t) - \alpha_2 T(z_1(t)) \end{cases} \tag{6}$$

$$\begin{cases} \psi_{tt}(x,t) = \tilde{c}_a^2 \psi_{xx}(x,t) - \gamma_a \psi_t(x,t) \\ \psi_x(0,t) = \tilde{h}\psi_t(0,t) - \tilde{u}_2(t) \\ \psi_t(1,t) = y_1(t) \\ \dot{y}_1(t) = -\beta_1 \psi_x(1,t) - \beta_2 T(z_1(t)) \end{cases} \tag{7}$$

where the normalized parameters are given in Table III. Note that the range for the spacial variable is now $x \in [0, 1]$ to ease the calculations. The initial conditions are as follows:

$$\begin{cases} \phi(x,0) = \phi^0(x), & \phi_t(x,0) = \phi^1(x) \\ \psi(x,0) = \psi^0(x), & \psi_t(x,0) = \psi^1(x) \\ z_1(0) = \phi^1(1), & y_1(0) = \psi^1(1). \end{cases}$$

Since the existence and uniqueness of a solution to the previous problem is not the main contribution of this article, it is assumed in the sequel. This problem has been widely studied

TABLE III
Normalized Parameters

Parameter	Expression	Value
$\phi(x,t)$	$\Phi(xL,t)$	-
$\psi(x,t)$	$\Psi(xL,t)$	-
$\tilde{c}_t$	$c_t L^{-1}$	1.57
$\tilde{c}_a$	$c_a L^{-1}$	2.5
α_1	$\frac{GJ}{LI_B}$	5.3
β_1	$\frac{E\Gamma}{LM_B}$	8.75
α_2	I_B^{-1}	$1.12 \cdot 10^{-2}$
β_2	$\frac{\delta}{M_B}$	$2.5 \cdot 10^{-5}$
$\tilde{g}$	$\frac{g}{GJ}$	$2.1 \cdot 10^{-3}$
$\tilde{h}$	$\frac{h}{E\Gamma}$	$2.86 \cdot 10^{-7}$
$\tilde{u}_1(t)$	$\frac{1}{GJ}u_1(t)$	-
$\tilde{u}_2(t)$	$\frac{1}{E\Gamma}u_2(t)$	-

(see [10], [12], [37], [39], [44] among many others), and the solution belongs to the following space if the initial conditions (ϕ^0, ϕ^1, ψ^0, and ψ^1) satisfy the boundary conditions (see [9] for more details):

$$\mathbb{X} = H^1 \times L^2, \quad \mathbb{X}_1 = H^2 \times H^1$$
$$(\phi, \phi_t, \psi, \psi_t, z_1, y_1) \in C^0\big(\mathbb{X}_1^2 \times \mathbb{R}^2\big).$$

Remark 1: One may note that $\theta \mapsto T_{nl}(\theta)$ is not well defined for $\theta = 0$ because of the sign function. Nevertheless, since the nonlinearity acts directly on the variable z, it follows that there exists a unique solution to the ODE system in the sense of Filipov [19]. A more detailed discussion on this point is provided in [11]. □

Systems (6) and (7) is a cascade of two subsystems.

1) System (6) is a coupled nonlinear ODE/string equation describing the torsion angle ϕ.
2) System (7) is a coupled linear ODE/string equation subject to the external perturbation $T(z_1)$ for Ψ.

It appears clearly that the perturbation on the second subsystem depends on the first subsystem in ϕ. Since they are very similar, the same analysis than the one conducted in this article applies for the second subproblem. That is why we only study the evolution of the torsion.

IV. Exponential Stability of the Linear System

System (6) is a nonlinear system because of the friction term T_{nl} introduced in (2). Nevertheless, for a high-desired angular speed Ω_0, T_{nl} can be assumed constant, as seen in Fig. 3. Moreover, studying this linear system can be seen as a first

step before studying the nonlinear system, which relies mostly on the stability theorem derived in this section.

The proposed linear model of T around $\Omega_0 \gg 1$ is

$$T(\theta) = c_b\theta + T_{nl}(\Omega_0) = c_b\theta + T_0. \tag{8}$$

For high values of Ω_0, $T_0 = T_{nl}(\Omega_0)$ is close to $T_{smooth}(\Omega_0)$, and at the limit when Ω_0 tends to infinity, they are equal. Hence, the nonlinear friction term for relatively large angular velocity does not influence much the system.

In our case, the proposed controller for this problem has been studied in a different setting in [13], [15], and [45] and is a simple proportional/integral controller based on the single measurement of the angular velocity at the top of the drill (i.e., $\phi_t(0,t)$). The following variables are, therefore, introduced:

$$\begin{aligned} \tilde{u}_1(t) &= -k_p(\phi_t(0,t) - \Omega_0) - k_i z_2(t) \\ \dot{z}_2(t) &= \phi_t(0,t) - \Omega_0 \end{aligned} \tag{9}$$

where k_p and k_i are the gains of the PI controller. Combining (6), (8), and (9) leads to

$$\begin{cases} \phi_{tt}(x,t) = c^2\phi_{xx}(x,t) - \gamma_t\phi_t(x,t) \\ \phi_x(0,t) = (\tilde{g} + k_p)\phi_t(0,t) - k_p\Omega_0 + k_i C_2\ Z(t) \\ \phi_t(1,t) = C_1 Z(t) \\ \dot{Z}(t) = AZ(t) + B\begin{bmatrix} \phi_t(0,t) \\ \phi_x(1,t) \end{bmatrix} + B_2\begin{bmatrix} \Omega_0 \\ T_0 \end{bmatrix} \end{cases} \tag{10}$$

where

$$A = \begin{bmatrix} -\dfrac{c_b}{I_B} & 0 \\ 0 & 0 \end{bmatrix},\quad B = \begin{bmatrix} 0 & -\alpha_1 \\ 1 & 0 \end{bmatrix},\ B_2 = \begin{bmatrix} 0 & -\alpha_2 \\ -1 & 0 \end{bmatrix}$$

$$Z = \begin{bmatrix} z_1 & z_2 \end{bmatrix}^\top,\quad C_1 = \begin{bmatrix} 1 & 0 \end{bmatrix},\ C_2 = \begin{bmatrix} 0 & 1 \end{bmatrix}.$$

To ease the notations, $c = \tilde{c}_t$. We denote by

$$X = (\phi_x, \phi_t, z_1, z_2) \in C^1([0,\infty), \mathcal{H})$$

with $\mathcal{H} = L^2 \times L^2 \times \mathbb{R}^2$ the infinite-dimensional state of system (10). The control objective in the linear case is to achieve the exponential stabilization of an equilibrium point of (10) in angular speed, i.e., $\phi_t(1)$ is going exponentially to a given constant reference value Ω_0. To this extent, the following norm on $\mathcal{H}$ is introduced:

$$\|X\|_{\mathcal{H}}^2 = z_1^2 + z_2^2 + c^2\|\phi_x(\cdot)\|^2 + \|\phi_t(\cdot)\|^2.$$

The definition of an equilibrium point of (10) and its exponential stability follows from the earlier definitions.

Definition 1: $X_\infty \in \mathcal{H}$ is an **equilibrium point** of (10) if for the trajectory $X \in C^1([0,\infty), \mathcal{H})$ of (10) with initial condition X_∞, the following holds:

$$\forall t > 0,\quad \|\dot{X}(t)\|_{\mathcal{H}} = 0.$$

Definition 2: Let X_∞ be an equilibrium point of (10). X_∞ is said to be μ **exponentially stable** if

$$\forall t > 0,\quad \|X(t) - X_\infty\|_{\mathcal{H}} \le \gamma\ \|X_0 - X_\infty\|_{\mathcal{H}}\ e^{-\mu t}$$

holds for $\gamma \geqslant 1$, $\mu > 0$ and for any initial conditions $X_0 \in \mathcal{H}$ satisfying the boundary conditions. Here, X is the trajectory of (10) whose initial condition is X_0.

Hence, X_∞ is said to be **exponentially stable** if there exists $\mu > 0$ such that X_∞ is μ exponentially stable.

Before stating the main result of this part, a lemma about the equilibrium point is proposed.

Lemma 1: Assume $k_i \neq 0$, then there exists a unique equilibrium point $X_\infty = (\phi_x^\infty, \phi_t^\infty, z_1^\infty, z_2^\infty) \in \mathcal{H}$ of (10) and it satisfies $\phi_t^\infty = \Omega_0$.

Proof: An equilibrium point X_∞ of (10) is such that: $(\phi_{xt}^\infty, \phi_{tt}^\infty, (d/dt)z_1^\infty, (d/dt)z_2^\infty) = 0$.

Since $(d/dt)z_2^\infty = \phi_t^\infty(0,t) - \Omega_0 = 0$ and $\partial_x\phi_t^\infty = 0$ and $\partial_t\phi_t^\infty = 0$, $\phi_t^\infty = \Omega_0$ holds.

We also get from $\phi_{xx}^\infty = 0$ and $\partial_t\phi_x^\infty = 0$ that ϕ_x^∞ is a first order polynomial in x. Together with the boundary conditions, this system has a unique solution if $k_i \neq 0$ such as:

$$X_\infty = \left(\phi_x^\infty, \Omega_0, \Omega_0, \frac{\phi_x^\infty(0) - \tilde{g}\Omega_0}{k_i}\right)$$

where $\phi_x^\infty(x) = (\gamma_t\Omega_0/c^2)(x-1) - (c_b/\alpha_1\ I_B)\Omega_0 - (\alpha_2/\alpha_1)T_0$ for $x \in [0,1]$. ■

A. Exponential Stability of the Closed-Loop System (10)

The main result of this part is then stated as follows.

Theorem 1: Let $N \in \mathbb{N}$. Assume there exists $P_N \in \mathbb{S}^{2+2(N+1)}$, $R = \operatorname{diag}(R_1, R_2) \succeq 0$, $S = \operatorname{diag}(S_1, S_2) \succ 0$, $Q \in \mathbb{S}_+^2$ such that the following LMIs hold:

$$\begin{aligned} \Theta_N &= c\ \Theta_{1,N} + \Theta_{2,N} - Q_N \prec 0 \\ P_N + S_N &\succ 0 \end{aligned} \tag{11}$$

and

$$\begin{aligned} \Gamma_0 &= cR + \frac{\gamma_t}{2}U_0 - Q \succeq 0 \\ \Gamma_1 &= cR + \frac{\gamma_t}{2}U_1 - Q \succeq 0 \end{aligned} \tag{12}$$

where

$$\begin{aligned} \Theta_{1,N} &= H_N^\top \begin{bmatrix} S_1 + R_1 & 0 \\ 0 & -S_2 \end{bmatrix} H_N - G_N^\top \begin{bmatrix} S_1 & 0 \\ 0 & -S_2 - R_2 \end{bmatrix} G_N \\ \Theta_{2,N} &= \operatorname{He}\left(D_N^\top P_N F_N\right) \\ F_N &= [I_{2+2(N+1)} \quad 0_{2+2(N+1),2}] \\ D_N &= \begin{bmatrix} J_N^\top & cM_N^\top \end{bmatrix}^\top,\quad J_N = [A \quad 0_{2,2(N+1)} \quad B] \\ M_N &= \mathbb{1}_N H_N - \bar{\mathbb{1}}_N G_N - \begin{bmatrix} 0_{2(N+1),2} & L_N & 0_{2(N+1),2} \end{bmatrix} \\ U_0 &= \begin{bmatrix} 2\ S_1 & S_1 + S_2 + R_2 \\ S_1 + S_2 + R_2 & 2(S_2 + R_2) \end{bmatrix} \\ U_1 &= \begin{bmatrix} 2(S_1 + R_1) & S_1 + S_2 + R_1 \\ S_1 + S_2 + R_1 & 2\ S_2 \end{bmatrix} \\ G_N &= \begin{bmatrix} ck_iC_2 & 0_{2,2(N+1)} & G \end{bmatrix},\quad G = \begin{bmatrix} 1 + c(\tilde{g} + k_p) & 0 \\ 1 - c(\tilde{g} + k_p) & 0 \end{bmatrix} \\ H_N &= \begin{bmatrix} C_1 & 0_{2,2(N+1)} & H \end{bmatrix},\quad H = \begin{bmatrix} 0 & c \\ 0 & -c \end{bmatrix} \\ Q_N &= \operatorname{diag}(0_2, Q, 3\ Q, \ldots, (2N+1)Q, 0_2) \\ S_N &= \operatorname{diag}(0_2, S, 3S, \ldots, (2N+1)S) \\ L_N &= \left[\ell_{j,k}\Lambda\right]_{j,k\in[0,N]} - \frac{\gamma_t}{2}\operatorname{diag}\left(\begin{bmatrix} 1 & 1 \\ 1 & 1 \end{bmatrix}, \ldots, \begin{bmatrix} 1 & 1 \\ 1 & 1 \end{bmatrix}\right) \end{aligned}$$

$$\mathbb{1}_N = \begin{bmatrix} \Lambda \\ \vdots \\ \Lambda \end{bmatrix}, \quad \bar{\mathbb{1}}_N = \begin{bmatrix} \Lambda \\ \vdots \\ (-1)^N \Lambda \end{bmatrix}, \quad \Lambda = \begin{bmatrix} c & 0 \\ 0 & -c \end{bmatrix} \tag{13}$$

and

$$\ell_{k,j} = \begin{cases} (2j+1)(1-(-1)^{j+k}), & \text{if } j \leqslant k \\ 0, & \text{otherwise} \end{cases}$$

then the equilibrium point of system (10) is exponentially stable. As a consequence, $\lim_{t\to+\infty} |\phi_t(1,t) - \Omega_0| = 0$.

The proof is given thereafter, but some practical consequences and preliminary results are derived first.

Remark 2: The methodology used to derive the previous result has been introduced first in [42] to deal with time-delay systems. It has been proven in the former article that this theorem provides a hierarchy of LMI conditions. That means if the conditions of Theorem 1 are met for $N = N_1 \geqslant 0$, and then the conditions are also satisfied for all $N > N_1$. Then, the LMIs provide a sharper analysis as the order N of the theorem increases. Nevertheless, the price to pay for a more precise analysis is the increase in the number of decision variables and consequently a higher computational burden. It has been noted in [42] for a time-delay system and in [8] for a coupled ODE/string equation system that very sharp results are obtained even for low orders N. □

As we aim at showing that X_∞ is an exponentially stable equilibrium point of system (10) in the sense of Definition 2, the following variable is consequently defined for $t \geq 0$:

$$\tilde{X}(t) = X(t) - X_\infty = (\tilde{\phi}_x(t), \tilde{\phi}_t(t), \tilde{z}_1(t), \tilde{z}_2(t))$$

where X is a trajectory of system (10).

The following lemma, given in [7], provides a way for estimating the exponential decay rate of system (10) as soon as a Lyapunov functional V is known.

Lemma 2: Let V be a Lyapunov functional for system (10) and $\mu \geq 0$. Assume there exist $\varepsilon_1, \varepsilon_2, \varepsilon_3 > 0$ such that the following holds:

$$\begin{cases} \varepsilon_1 \|\tilde{X}\|^2_{\mathcal{H}} \leqslant V(\tilde{X}) \leqslant \varepsilon_2 \|\tilde{X}\|^2_{\mathcal{H}} \\ \dot{V}(\tilde{X}) + 2\mu V(\tilde{X}) \leqslant -\varepsilon_3 \|\tilde{X}\|^2_{\mathcal{H}} \end{cases} \tag{14}$$

then the equilibrium point of system (10) is μ exponentially stable. If $\mu = 0$, then it is exponentially stable.

Proof of Theorem 1: For simplicity, the following notations are used throughout this article for $k \in \mathbb{N}$:

$$\tilde{\chi}(x) = \begin{bmatrix} \tilde{\phi}_t(x) + c\tilde{\phi}_x(x) \\ \tilde{\phi}_t(x) - c\tilde{\phi}_x(x) \end{bmatrix}, \quad \tilde{\mathfrak{X}}_k(t) = \int_0^1 \tilde{\chi}(x,t)\mathcal{L}_k(x)dx \tag{15}$$

where $\{\mathcal{L}_k\}_{k\in\mathbb{N}}$ is the orthogonal family of Legendre polynomials as defined in Appendix. $\tilde{\mathfrak{X}}_k$ is then the projection coefficient of $\tilde{\chi}$ along the Legendre polynomial of degree k. $\tilde{\chi}$ refers to the Riemann coordinates and presents useful properties as discussed in [8] for instance.

1) Choice of a Lyapunov Functional Candidate: The proposed Lyapunov functional is inspired from [7], [8], and [36] and is divided into two parts as follows:

$$V_N(\tilde{X}) = \tilde{Z}_N^\top P_N \tilde{Z}_N + \mathcal{V}(\tilde{\chi}) \tag{16}$$

where $\tilde{Z}_N = [\tilde{z}_1 \ \tilde{z}_2 \ \tilde{\mathfrak{X}}_0^\top \ \cdots \ \tilde{\mathfrak{X}}_N^\top]^\top$ and

$$\mathcal{V}(\tilde{\chi}) = \int_0^1 \tilde{\chi}^\top(x) \begin{bmatrix} S_1 + xR_1 & 0 \\ 0 & S_2 + (1-x)R_2 \end{bmatrix} \tilde{\chi}(x)dx.$$

$\mathcal{V}$ is a traditional Lyapunov functional candidate for a transport system, as shown in [16].

2) Exponential Stability: Existence of ε_1: This part is inspired by [7]. The inequalities $P_N + S_N \succ 0$, $R \succeq 0$ imply the existence of $\varepsilon_1 > 0$ such that

$$P_N + S_N \succeq \varepsilon_1 \text{diag}\left(I_2, \frac{1}{2}\mathcal{I}_N\right)$$
$$S \succeq \frac{\varepsilon_1}{2} I_2 \tag{17}$$

with $\mathcal{I}_N = \text{diag}\{(2k+1)I_2\}_{k\in[0,N]}$. This statement implies the following on V_N:

$$\begin{aligned} V_N(\tilde{X}) &\geq \tilde{Z}_N^\top (P_N + S_N)\tilde{Z}_N - \sum_{k=0}^{N}(2k+1)\tilde{\mathfrak{X}}_k^\top S \tilde{\mathfrak{X}}_k \\ &\quad + \int_0^1 \tilde{\chi}(x)^\top \left(S - \frac{\varepsilon_1}{2} I_2\right)\tilde{\chi}(x)dx + \frac{\varepsilon_1}{2}\|\tilde{\chi}\|^2 \\ &\geq \varepsilon_1 \left(\tilde{z}_1^2 + \tilde{z}_2^2 + \frac{1}{2}\|\tilde{\chi}\|^2\right) \\ &\quad - \sum_{k=0}^{N}(2k+1)\tilde{\mathfrak{X}}_k^\top \tilde{S}\tilde{\mathfrak{X}}_k + \int_0^1 \tilde{\chi}^\top(x)\tilde{S}\tilde{\chi}(x)dx \\ &\geq \varepsilon_1 \|\tilde{X}\|^2_{\mathcal{H}} \end{aligned}$$

where $\tilde{S} = S - (\varepsilon_1/2)I_2$ which ends the proof of existence of ε_1.

Existence of ε_2: Following the same line as earlier, the following holds for a sufficiently large $\varepsilon_2 > 0$:

$$P_N \preceq \varepsilon_2 \text{diag}\left(I_2, \frac{1}{4}\mathcal{I}_N\right)$$
$$\frac{\varepsilon_2}{4} I_2 \succeq \begin{bmatrix} S_1 + xR_1 & 0 \\ 0 & S_2 + (1-x)R_2 \end{bmatrix}.$$

Using these inequalities in (16) leads to

$$\begin{aligned} V_N(\tilde{X}) &\leq \varepsilon_2 \left(\tilde{z}_1^2 + \tilde{z}_2^2 + \sum_{k=0}^{N}\frac{2k+1}{4}\tilde{\mathfrak{X}}_k^\top \tilde{\mathfrak{X}}_k + \frac{1}{4}\|\tilde{\chi}\|^2\right) \\ &\leq \varepsilon_2 \left(\tilde{z}_1^2 + \tilde{z}_2^2 + \frac{1}{2}\|\tilde{\chi}\|^2\right) = \varepsilon_2 \|\tilde{X}\|^2_{\mathcal{H}}. \end{aligned}$$

The last inequality is a direct application of Lemma 4.

Existence of ε_3: The time derivation of $\tilde{\chi}$ leads to

$$\tilde{\chi}_t(x) = \Lambda \tilde{\chi}_x(x) - \gamma_t \begin{bmatrix} 1 \\ 1 \end{bmatrix} \tilde{\phi}_t(x).$$

Noting that $\tilde{\phi}_t(x) = (1/2)[1 \ 1]\tilde{\chi}(x)$, we get

$$\tilde{\chi}_t(x) = \Lambda \tilde{\chi}_x(x) - \frac{\gamma_t}{2}\begin{bmatrix} 1 & 1 \\ 1 & 1 \end{bmatrix}\tilde{\chi}(x). \tag{18}$$

The derivative of $\mathcal{V}$ along the trajectories of (6) leads to

$$\dot{\mathcal{V}}(\tilde{\chi}) = 2c\mathcal{V}_1(\tilde{\chi}) - \frac{\gamma_t}{2}\mathcal{V}_2(\tilde{\chi})$$

with

$$\mathcal{V}_1(\tilde{\chi}) = \int_0^1 \tilde{\chi}_x^\top(x) \begin{bmatrix} S_1 + xR_1 & 0 \\ 0 & -S_2 - (1-x)R_2 \end{bmatrix} \tilde{\chi}(x)dx$$

$$\mathcal{V}_2(\tilde{\chi}) = \int_0^1 \tilde{\chi}^\top(x) U(x) \tilde{\chi}(x) dx$$
$$U(x) = \begin{bmatrix} 2(S_1 + xR_1) & S_1 + S_2 + xR_1 + (1-x)R_2 \\ S_1 + S_2 + xR_1 + (1-x)R_2 & 2(S_2 + (1-x)R_2) \end{bmatrix}.$$

An integration by part on $\mathcal{V}_1$ shows that

$$\begin{aligned} 2\mathcal{V}_1(\tilde{\chi}) = {} & \tilde{\chi}^\top(1) \begin{bmatrix} S_1 + R_1 & 0 \\ 0 & -S_2 \end{bmatrix} \tilde{\chi}(1) \\ & - \tilde{\chi}^\top(0) \begin{bmatrix} S_1 & 0 \\ 0 & -S_2 - R_2 \end{bmatrix} \tilde{\chi}(0) \\ & - \int_0^1 \tilde{\chi}^\top(x) \begin{bmatrix} R_1 & 0 \\ 0 & R_2 \end{bmatrix} \tilde{\chi}(x) dx. \end{aligned}$$

The previous calculations lead to the following derivative:

$$\begin{aligned} \dot{\mathcal{V}}(\tilde{\chi}) = {} & c \left(\tilde{\chi}^\top(1) \begin{bmatrix} S_1 + R_1 & 0 \\ 0 & -S_2 \end{bmatrix} \tilde{\chi}(1) \right. \\ & \left. - \tilde{\chi}^\top(0) \begin{bmatrix} S_1 & 0 \\ 0 & -S_2 - R_2 \end{bmatrix} \tilde{\chi}(0) \right) \\ & - \int_0^1 \tilde{\chi}^\top(x) \left(cR + \frac{\gamma_t}{2} U(x) \right) \tilde{\chi}(x) dx. \end{aligned} \quad (19)$$

By a convexity argument, if (12) is verified, then $cR + U(x) \geq Q \succ 0$ holds for $x \in [0, 1]$. Consequently, noticing that $\tilde{\chi}(0) = G_N \tilde{\xi}_N$, $\tilde{\chi}(1) = H_N \tilde{\xi}_N$, we get

$$\dot{\mathcal{V}}(\tilde{\chi}) \leq c \tilde{\xi}_N^\top \Theta_{1,N} \tilde{\xi}_N - \int_0^1 \tilde{\chi}^\top(x) Q \tilde{\chi}(x) dx$$

with

$$\tilde{\xi}_N = \begin{bmatrix} \tilde{Z}_N^\top & \tilde{\phi}_t(0) & \tilde{\phi}_x(1) \end{bmatrix}^\top.$$

Using Lemma 5 and the fact that $\dot{\tilde{Z}}_N = D_N \tilde{\xi}_N$ and $\tilde{Z}_N = F_N \tilde{\xi}_N$, we get the following:

$$\begin{aligned} \dot{V}_N(\tilde{X}) = {} & \mathrm{He}\left(\dot{\tilde{Z}}_N^\top P_N \tilde{Z}_N \right) + \dot{\mathcal{V}}(\tilde{\chi}) \\ \leq {} & \tilde{\xi}_N^\top \Theta_N \tilde{\xi}_N + \sum_{k=0}^{N} (2k+1) \tilde{\mathfrak{X}}_k Q \tilde{\mathfrak{X}}_k \\ & - \int_0^1 \tilde{\chi}^\top(x) Q \tilde{\chi}(x) dx \end{aligned} \quad (20)$$

with Θ_N defined in (11). Since $\Theta_N \prec 0$ and $Q \succ 0$, we get

$$\begin{aligned} \Theta_N \preceq {} & -\varepsilon_3 \mathrm{diag}\left(I_2, \frac{1}{2} I_2, \frac{3}{2} I_2, \ldots, \frac{2N+1}{2} I_2, 0_2 \right) \\ Q \succeq {} & \frac{\varepsilon_3}{2} I_2. \end{aligned}$$

Then, $\dot{V}_N$ is upper bounded by

$$\begin{aligned} \dot{V}_N(\tilde{X}) \leq {} & -\varepsilon_3 \left(\tilde{z}_1^2 + \tilde{z}_2^2 + \frac{1}{2} \|\tilde{\chi}\|^2 \right) \\ & + \sum_{k=0}^{N} (2k+1) \tilde{\mathfrak{X}}_k^\top \left(Q - \frac{\varepsilon_3}{2} I_2 \right) \tilde{\mathfrak{X}}_k \\ & - \int_0^1 \tilde{\chi}^\top(x) \left(Q - \frac{\varepsilon_3}{2} I_2 \right) \tilde{\chi}(x) dx \\ \leq {} & -\varepsilon_3 \|\tilde{X}\|_{\mathcal{H}}^2. \end{aligned}$$

The last inequality comes from a direct application of Bessel's inequality (31).

Conclusion: Using Lemma 2, we indeed get the exponential convergence of all trajectories of (10) to the desired equilibrium point.

B. Exponential Stability With a Guaranteed Decay Rate

It is possible to estimate the decay rate μ of the exponential convergence with a slight modification of the LMIs as it is proposed in the following corollary.

Corollary 1: Let $N \in \mathbb{N}$, $\mu > 0$ and $\gamma_t \geq 0$. If there exist $P_N \in \mathbb{S}^{2+2(N+1)}$, $R = \mathrm{diag}(R_1, R_2) \succeq 0$, $S = \mathrm{diag}(S_1, S_2) \succ 0$, *and* $Q \in \mathbb{S}_+^2$ such that (12) and the following LMIs hold:

$$\begin{aligned} \Theta_{N,\mu} = {} & \Theta_N + 2\mu F_N^\top (P_N + S_N) F_N \prec 0 \\ & 0 \prec P_N + S_N \end{aligned} \quad (21)$$

with the parameters defined as in Theorem 1, then the equilibrium point of system (10) is μ exponentially stable.

Proof: To prove the exponential stability with a decay rate of at least $\mu > 0$, we use Lemma 2. Similar to the previous proof, we have the existence of ε_1 and $\varepsilon_2 > 0$. The existence of ε_3 is slightly different. First, note that for the Lyapunov functional candidate (16), we get

$$\begin{aligned} V_N(\tilde{X}_\phi) \geq {} & \tilde{Z}_N^\top P_N \tilde{Z}_N + \int_0^1 \tilde{\chi}^\top(x) S \tilde{\chi}(x) dx \\ \geq {} & \tilde{Z}_N^\top P_N \tilde{Z}_N + \sum_{k=0}^{N} (2k+1) \tilde{\mathfrak{X}}_k^\top S \tilde{\mathfrak{X}}_k. \end{aligned}$$

This inequality was obtained using (31). Using the notations of the previous theorem yields

$$V_N(\tilde{X}_\phi) \geq \tilde{\xi}_N^\top F_N^\top (P_N + S_N) F_N \tilde{\xi}_N. \quad (22)$$

Coming back to (20) and using (21) leads to:

$$\begin{aligned} \dot{V}_N(\tilde{X}_\phi) \leq {} & \tilde{\xi}_N^\top \Theta_{N,\mu} \tilde{\xi}_N - 2\mu \tilde{\xi}_N^\top \left(F_N^\top P_N F_N + S_N \right) \tilde{\xi}_N \\ & + \sum_{k=0}^{N} (2k+1) \tilde{\mathfrak{X}}_k^\top Q \tilde{\mathfrak{X}}_k - \int_0^1 \tilde{\chi}^\top(x) Q \tilde{\chi}(x) dx. \end{aligned}$$

Injecting inequality (22) into the previous inequality leads to

$$\begin{aligned} \dot{V}_N(\tilde{X}_\phi) + 2\mu V_N(\tilde{X}_\phi) \leq {} & \tilde{\xi}_N^\top \Theta_{N,\mu} \tilde{\xi}_N + \sum_{k=0}^{N} (2k+1) \tilde{\mathfrak{X}}_k^\top Q \tilde{\mathfrak{X}}_k \\ & - \int_0^1 \tilde{\chi}^\top(x) Q \tilde{\chi}(x) dx. \end{aligned}$$

Using the same techniques than for the previous proof leads to the existence of $\varepsilon_3 > 0$ such that

$$\dot{V}_N(\tilde{X}_\phi) + 2\mu V_N(\tilde{X}_\phi) \leq -\varepsilon_3 \|\tilde{X}_\phi\|_{\mathcal{H}}^2.$$

Lemma 2 concludes then on the μ-exponential stability. ■

Remark 3: Wave equations can sometimes be modeled as neutral time-delay systems [6], [38]. This kind of system is known to possess some necessary stability conditions as noted in [6] and [9]. In [9], the following criterion is derived:

$$\mu \leq \frac{c}{2} \log \left| \frac{1 + c(\tilde{g} + k_p)}{1 - c(\tilde{g} + k_p)} \right| = \mu_{\max}. \quad (23)$$

This result implies that there exists a maximum decay rate, and if this maximum is negative, then the system is unstable. The LMI $\Theta_N^\mu \prec 0$ contains the same necessary condition, meaning that the neutral aspect of the system is well captured. □

C. Strong Stability Against Small Delay in the Control

A practical consequence of the neutral aspect of system (10) is that it is very sensitive to delay in the control (9). Indeed, if the control is slightly delayed, a new necessary stability condition [equivalent to (23)] coming from frequency analysis can be derived [21, Corollary 3.3]

$$\left|\frac{1-c\tilde{g}}{1+c\tilde{g}}\right| + 2\left|\frac{ck_p}{1+c\tilde{g}}\right| < 1.$$

It is more restrictive and taking $k_p \neq 0$ practically leads to a decrease of the robustness (even if some other performances might be enhanced). This phenomenon has been studied in many articles [22], [29], [44]. Hence, to be robust to delays in the loop, one then needs to ensure the following:

$$0 \leq k_p \leq \frac{1}{2c}\left(|1+c\tilde{g}| - |1-c\tilde{g}|\right) = \tilde{g} = 2.1 \cdot 10^{-3}.$$

This inequality on k_p comes when considering the infinite-dimensional problem and does not arise when dealing with any finite-dimensional model. That point enlightens that it is more realistic to consider the infinite-dimensional problem. For more information on that point, the interested reader can refer to [5].

V. Practical Stability of System (6)–(9)

The experiments conducted previously show for Ω_0 large, the trajectory of the nonlinear system (6)–(9) goes exponentially to X_∞, so does the linear system. In other words, the previous result is a local stability test for the nonlinear system in case of large-desired angular velocity Ω_0 and does not extend straightforwardly to a global analysis.

In general, for a nonlinear system, ensuring the global exponential stability of an equilibrium point could be complicated. In many engineering situations, global exponential stability is not the requirement. Indeed, considering uncertainties in the system or nonlinearities, it is far more reasonable and acceptable for engineers to ensure that the trajectory remains close to the equilibrium point. This property is called dissipativeness in the sense of Levinson [26] or practical stability (also called globally uniformly ultimately bounded in [24]).

Definition 3: System (6) is **practically stable** if there exists $X_{\text{bound}} \geq 0$ such that for X the solution of (6) with initial condition $X_0 \in \mathcal{H}$

$$\forall \eta > 0, \quad \exists T_\eta > 0 \ \forall t \geq T_\eta, \ \ \|X(t) - X_\infty\|_{\mathcal{H}} \leq X_{\text{bound}} + \eta. \quad (24)$$

Saying that system (6)–(9) is practically stable means that there exists $T_\eta > 0$ such that for any $x \in [0,1]$, $\phi_t(x,t)$ stays close to Ω_0 for $t \geq T_\eta$. This property has already been applied to a drilling system in [39] for instance. In the nonlinear case, the aim is then to design a control law reducing the amplitude of the stick-slip when it occurs.

The objective of this section is to derive an LMI test ensuring the practical stability of nonlinear system (6) together with the control defined in (9)

$$\begin{cases} \phi_{tt}(x,t) = c^2\phi_{xx}(x,t) - \gamma_t\phi_t(x,t) \\ \phi_x(0,t) = (\tilde{g}+k_p)\phi_t(0,t) - k_p\Omega_0 + k_iC_2\ Z(t) \\ \phi_t(1,t) = C_1Z(t) \\ \dot{Z}(t) = AZ(t) + B\begin{bmatrix}\phi_t(0,t)\\ \phi_x(1,t)\end{bmatrix} + B_2\begin{bmatrix}\Omega_0\\ T_{nl}(z_1(t))\end{bmatrix}. \end{cases} \quad (25)$$

Remark 4: To simplify the writing, ϕ can both means the solution of the linear or nonlinear system depending on the context. In this part, it refers to a solution of nonlinear system (25). □

A. Practical Stability of System (25)

The idea behind practical stability is to embed the static nonlinearities by the use of suitable sector conditions, as it has been done for the saturation, for instance [43]. Then, the use of robust tools will lead to some LMI tests ensuring the practical stability.

Lemma 3: For almost all $\tilde{z}_1 \in \mathbb{R}$, the following holds:

$$\begin{aligned} T_{nl}(\tilde{z}_1+\Omega_0)^2 \leq T_{\max}^2, \quad T_{\min}^2 \leq T_{nl}(\tilde{z}_1+\Omega_0)^2 \\ -2(\tilde{z}_1+\Omega_0)T_{nl}(\tilde{z}_1+\Omega_0) \leq 0. \end{aligned} \quad (26)$$

Proof: These inequalities can be easily verified using (2). ■

This new information is the basis of the following theorem.

Theorem 2: Let $N \in \mathbb{N}$ and $V_{\max} > 0$. If there exist $P_N \in \mathbb{S}^{2+2(N+1)}$, $R = \text{diag}(R_1, R_2) \succeq 0$, $S = \text{diag}(S_1, S_2) \succ 0$, *and* $Q \in \mathbb{S}_+^2$, $\tau_0, \tau_1, \tau_2, \tau_3 \geq 0$ such that (12) holds together with:

$$\begin{aligned} \Xi_N &= \bar{\Theta}_N - \tau_0\Pi_0 - \tau_1\Pi_1 - \tau_2\Pi_2 - \tau_3\Pi_3 \prec 0 \\ 0 &\prec P_N + S_N \end{aligned} \quad (27)$$

where

$$\begin{aligned} \bar{\Theta}_N &= \text{diag}(\Theta_N, 0_2) - \alpha_2\text{He}\big((F_{m1} - T_0\ F_{m2})^\top e_1^\top P_N\tilde{F}_N\big) \\ \tilde{F}_N &= [F_N \quad 0_{2(N+1)+2,2}], \quad e_1 = [1 \quad 0_{1,2(N+1)+1}]^\top, \\ F_{m1} &= [0_{1,2(N+1)+4} \quad 1 \quad 0], \quad F_{m2} = [0_{1,2(N+1)+4} \quad 0 \quad 1] \\ \Pi_0 &= V_{\max}F_{m2}^\top F_{m2} - \tilde{F}_N^\top(P_N+S_N)\tilde{F}_N \\ \Pi_1 &= \pi_2^\top\pi_2 - T_{\max}^2\pi_3^\top\pi_3, \quad \Pi_2 = T_{\min}^2\pi_3^\top\pi_3 - \pi_2^\top\pi_2 \\ \Pi_3 &= -\text{He}((\pi_1+\Omega_0\pi_3)^\top\pi_2) \\ \pi_1 &= [1, 0_{1,2(N+1)+3}, 0, 0], \quad \pi_2 = [0_{1,2(N+1)+4}, 1, 0] \\ \pi_3 &= [0_{1,2(N+1)+4}, 0, 1] \end{aligned}$$

and all the parameters defined as in Theorem 1, then the equilibrium point X_∞ of system (25) is practically stable. More precisely, (24) holds for $X_{\text{bound}} = (V_{\max}\varepsilon_1^{-1})^{1/2}$ where ε_1 is defined in (17).

Proof: First, let us do the same change of variable as before

$$\tilde{X} = X - X_\infty.$$

Since the nonlinearity affects only the ODE part of system (25), the difference with the previous part lies in the dynamic of $\tilde{Z}$:

$$\dot{\tilde{Z}}(t) = \frac{d}{dt}\left(Z(t) - \begin{bmatrix} z_1^\infty \\ z_2^\infty \end{bmatrix}\right) = A\tilde{Z}(t) + B\begin{bmatrix}\tilde{\phi}_t(0,t) \\ \tilde{\phi}_x(1,t)\end{bmatrix} + B_2\begin{bmatrix} 0 \\ T_{nl}(\tilde{z}_1(t)+\Omega_0) - T_0\end{bmatrix}.$$

Using the same Lyapunov functional as in (16), the positivity is ensured in exactly the same way. For the bound on the time derivative, following the same strategy as before, we easily get:

$$\dot{V}_N(\tilde{X}) \leq \tilde{\xi}_N^\top \Theta_N \tilde{\xi}_N - 2\alpha_2(T_{nl}(\tilde{z}_1+\Omega_0)-T_0)e_1^\top P_N \tilde{Z}_N + \sum_{k=0}^{N}(2k+1)\tilde{\mathfrak{X}}_k^\top Q\tilde{\mathfrak{X}}_k - \int_0^1 \tilde{\chi}^\top(x)Q\tilde{\chi}(x)dx. \quad (28)$$

We introduce a new extended state variable $\bar{\xi}_N = [\tilde{\xi}_N^\top \; T_{nl}(\tilde{z}_1+\Omega_0)\; 1]^\top$. Using the notation of Theorem 2, (28) rewrites as:

$$\dot{V}_N(\tilde{X}) \leq \bar{\xi}_N^\top \bar{\Theta}_N \bar{\xi}_N^\top + \sum_{k=0}^{N}(2k+1)\tilde{\mathfrak{X}}_k^\top Q\tilde{\mathfrak{X}}_k - \int_0^1 \tilde{\chi}^\top(x)Q\tilde{\chi}(x)dx.$$

It is impossible to ensure $\bar{\Theta}_N \prec 0$ since its last 2×2 diagonal block is 0_2.

We then use the definition of practical stability. We want to show that if there exists $\varepsilon_3 > 0$ such that $\dot{V}_N(\tilde{X}) \leq -\varepsilon_3\|\tilde{X}\|_{\mathcal{H}}^2$ when $V_N(\tilde{X}) \geq V_{\max}$ then the system is practically stable. Let $\mathcal{S} = \{\tilde{X} \in \mathcal{H} \mid V_N(\tilde{X}) \leq V_{\max}\}$, the previous assertion implies that this set is invariant and attractive. Using (17), we get that $\{\tilde{X} \in \mathcal{H} \mid \|\tilde{X}\|_{\mathcal{H}} \leq X_{\text{bound}} = V_{\max}^{1/2}\varepsilon_1^{-1/2}\} \supseteq \mathcal{S}$, meaning that the system is practically stable.

A sufficient condition to be practically stable is that V_N should be strictly decreasing when outside the ball of radius $V_{\max}$. This condition rewrites as $V_N(\tilde{X}) \geq V_{\max}$ and the following holds:

$$V_N(\tilde{X}) - V_{\max} \geq \tilde{Z}_N^\top P_N \tilde{Z}_N + \int_0^1 \tilde{\chi}^\top(x)S\tilde{\chi}(x)dx - V_{\max} \geq -\bar{\xi}_N^\top \Pi_0 \bar{\xi}_N \geq 0.$$

The previous inequality is obtained using Bessel inequality (31) on $\int_0^1 \tilde{\chi}^\top(x)S\tilde{\chi}(x)dx$. Hence, $V_N(\tilde{X}) \geq V_{\max}$ if $\bar{\xi}_N^\top \Pi_0 \bar{\xi}_N \leq 0$.

Noting that $\tilde{z}_1 = \pi_1\bar{\xi}_N$, $T_{nl}(\tilde{z}_1+\Omega_0) = \pi_2\bar{\xi}_N$ and $1 = \pi_3\bar{\xi}_N$, Lemma 3 rewrites as:

$$\forall i \in \{1,2,3\}, \quad \bar{\xi}_N \; \Pi_i \; \bar{\xi}_N \leq 0.$$

Consequently, a sufficient condition to be practically stable is:

$$\forall \bar{\xi}_N \neq 0 \text{ s. t. } \forall i \in [0,3], \quad \bar{\xi}_N^\top \Pi_i \bar{\xi}_N \leq 0, \; \bar{\xi}_N^\top \bar{\Theta}_N \bar{\xi}_N < 0. \quad (29)$$

The technique called *S-variable*, explained in [18] for instance, translates the previous inequalities into an LMI condition. Indeed, [18, Th. 1.1] shows that condition (29) is verified if there exists $\tau_0, \tau_1, \tau_2, \tau_3 > 0$ such that

$$\bar{\Theta}_N - \sum_{k=0}^{3}\tau_i\Pi_i \prec 0.$$

Consequently, in a similar way for Theorem 1, condition (27) implies that $\mathcal{S}$ is an invariant and attractive set for system (25). Then, the equilibrium point X_∞ of system (25) is practically stable with $X_{\text{bound}} = (V_{\max}\varepsilon_1^{-1})^{1/2}$. ■

Note that if the torque function is not perfectly known, one can change the lower and upper bounds $T_{\min}$ and $T_{\max}$ to get a more conservative result but robust to uncertainties on T_{nl}. For (27) to be feasible, the constraint $\bar{\xi}_N^\top \Pi_1 \bar{\xi}_N \leq 0$ must hold, meaning that an upper bound of T_{nl} needs to be proposed.

B. On the Optimization of X_{bound}

The condition (27) is a bilinear matrix inequality (BMI) since τ_0, τ_1, τ_2, and τ_3 are decision variables and it is, therefore, difficult to get its global optimum. Nevertheless, the following lemma gives a sufficient condition for the existence of a solution to this problem.

Corollary 2: There exists $V_{\max}$ and $\tau_0 > 0$ such that Theorem 2 holds if and only if there exists $N > 0$ such that LMIs (11) and (12) are satisfied.

In other words, the equilibrium point of system (25) is practically stable if and only if the linear system (10) is exponentially stable.

Proof: Note first that expending (27) with $\tau_3 = 0$ leads to

$$\Xi_N = \left[\begin{array}{c|cc} \Theta_{N,\tau_0/2} & \multicolumn{2}{c}{\kappa_{P_N}} \\ \hline & \tau_2-\tau_1 & 0 \\ \kappa_{P_N}^\top & \hline 0 & \tau_1 T_{\max}^2 - \tau_2 T_{\min}^2 \\ & & -\tau_0 V_{\max} \end{array}\right] \quad (30)$$

where $\kappa_{P_N} \in \mathbb{R}^{(4+2(N+1))\times 2}$ depends only on P_N.

Proof of Sufficiency: Assume there exists $N > 0$ such that LMIs (11) and (12) are satisfied. Considering $\tau_2 = 0$ and using Schur complement on Ξ_N, $\Xi_N \prec 0$ is equivalent to

$$\Theta_{N,\tau_0/2} - \kappa_{P_N}\begin{bmatrix} -\dfrac{1}{\tau_1} & 0 \\ 0 & \dfrac{1}{\tau_1 T_{\max}^2 - \tau_0 V_{\max}}\end{bmatrix}\kappa_{P_N}^\top \prec 0$$

with $\tau_0 V_{\max} > \tau_1 \; T_{\max}^2$. Since $\Theta_N \prec 0$, considering τ_0 small enough, τ_1 large and $V_{\max} > \tau_1\tau_0^{-1}T_{\max}^2$ the previous condition is always satisfied and Theorem 2 applies.

Proof of Necessity: Assume $\Xi_N \prec 0$ and (12) holds. Then, its first diagonal block must be definite negative. Consequently, $\Theta_N \prec 0$ and, according to Theorem 1, system (10) is exponentially stable. ■

Remark 5: Note that (30) provides a necessary condition for Theorem 2 which is $\Theta_{N,\tau_0/2} \prec 0$. In other words, τ_0 is related to the decay rate of the linear system, and we get the following condition: $\tau_0 < 2\mu_{\max}$. □

Thanks to Corollary 2, the following method should help solving the BMI if Theorem 1 is verified; assuming that (11) and (12) are verified for a given $N \in \mathbb{N}$.

1) Fix $\tau_0 = 2\mu_{\max}$ as defined in (23).
2) Check that (11), (12), and (27) are satisfied for $V_{\max}$ a strictly positive decision variable. If this is not the case, then decrease τ_0 and do this step again.
3) Thanks to Corollary 2, there exists a τ_0 small enough for which (11), (12), and (27) hold. Freeze this value.
4) Since the problem is unbounded, it is possible to fix a variable without loss of generality, let $V_{\max} = 10^4$ for instance and solve the following optimization problem:

$$\begin{aligned} \min_{P_N,S,R,Q,\tau_1,\tau_2,\tau_3,\varepsilon_P} \quad & -\varepsilon_P \\ & (11), (12) \text{ and } (27) \\ \text{s.t.} \quad & P_N + S_N - \operatorname{diag}(\varepsilon_P, 0_{2N+3}) \succ 0 \\ & R \succeq 0, \quad S \succ 0, \quad Q \succ 0. \end{aligned}$$

5) Then, compute $X_{\text{bound}} = (V_{\max}\varepsilon_1^{-1})^{1/2}$, where ε_1 is defined in (17).

VI. Examples and Simulations

This section is devoted to numerical simulations[2] and draw some conclusions about the PI regulation. In Section VI-A, we focus on the linear system and Section VI-B is dedicated to the nonlinear case.

A. On the Linear Model

This section recaps the result of the linear model.

1) Estimation of the Decay Rate: The main result is a direct application of Corollary 1 for $k_p = 10^{-3}$ and $k_i = 10$. Indeed, using a dichotomy-kind algorithm, Table IV is obtained. It shows the estimated decay rate μ at a given order between 0 and 6.

The first thing to note in Table IV is the hierarchy property, and the decay rate is an increasing function of the degree, as noted in Remark 2. Note also that the gap between order 0 and order 1 is significant, showing that using projections indeed improves the results.

For orders higher than 2, the estimated decay rate increases slightly, and, up to a four digits precision, it reaches its maximum value at $N = 6$. Since it is then the maximum allowable decay rate obtained using (23), it tends to show that the Lyapunov functional used in this article together with condition (21) are sharp and provide a good analysis. Fig. 5 represents a simulation on the linear system, and it confirms the same observation. Indeed, one can see that the energy of the system is well-bounded by an exponential curve and the bound becomes more and more accurate as N increases.

2) Stability of the Closed-Loop System: We are interested now in estimating the stability area in terms of the gains k_p and k_i such that the decay rate of the coupled system is $\mu_{\max}$ for an order $N = 5$. That leads to Fig. 6, where it is easy to see that increasing the gain k_p decreases the range of possible k_i while it increases its speed (see (23)). It is quite natural to note that the larger k_i is, the slower the system is, while increasing the proportional gain leads to a faster system. As a conclusion, for small values of k_p and k_i, the system is stable, and that was the conclusion of the two articles [44], [45] using a different Lyapunov functional. Note that with the earlier articles, it was not possible to quantify the notion of "small enough gains k_p and k_i" while it is possible to give an estimation with the method of this article.

[2]Numerical simulations are done using a first-order approximation with at least 80 space-discretization points and 9949 time-discretization points. Simulations are done using Yalmip [28] together with the SDP solver SDPT-3 [46]. The code is available at *https://homepages.laas.fr/mbarreau*.

TABLE IV

Estimated Decay Rate as a Function of the Order N Used. Note That $\mu_{\max} = 7.73 \cdot 10^{-3}$ is Calculated Using (23) for $k_p = 10^{-3}, k_i = 10$

Order	$N = 0$	$N = 1$	$N = 2$	$N = 3$	$N = 6$
μ $(\times 10^{-3})$	0.87	4.24	7.31	7.59	7.73

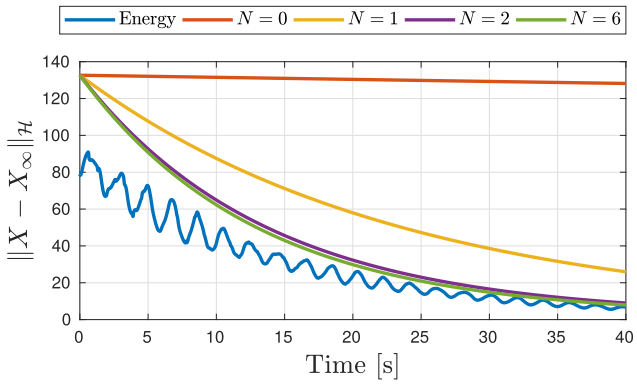

Fig. 5. Energy of X with the linear system for $k_p = 10^{-3}$, $k_i = 10$, and $\Omega_0 = 5$. The initial condition is $\phi^0(x) = 4(\int_0^x \phi_x^\infty(s)ds + 0.1\cos(2x))$, $\phi^1 = 2\Omega_0$, and $Z(0) = 2[z_1^\infty \; z_2^\infty]^\top$.

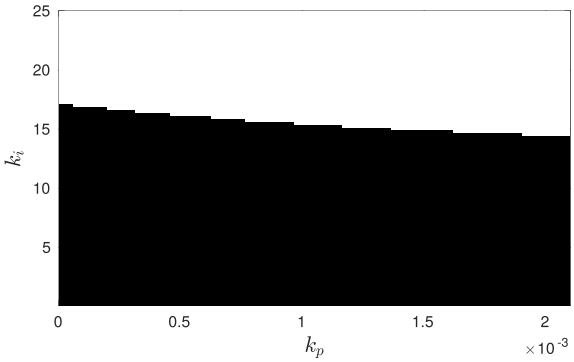

Fig. 6. Values of gains k_p and k_i leading to a stable system with the maximum decay rate for $N = 5$ using Theorem 1. The black area is stable, and the white area is said unstable up to an order 5.

B. Stick-Slip Effect on the Nonlinear Model

Section VI-A shows that the linear model is globally asymptotically stable for some values of gains k_p and k_i, and therefore, the nonlinear system (25) is locally asymptotically stable for a large-desired angular velocity Ω_0. This can been verified in Fig. 7(a) for $k_p = 10^{-3}$, $k_i = 10$, and $\Omega_0 = 10$. We can see that the linear and the nonlinear systems behave similarly if their initial condition is close to the equilibrium.

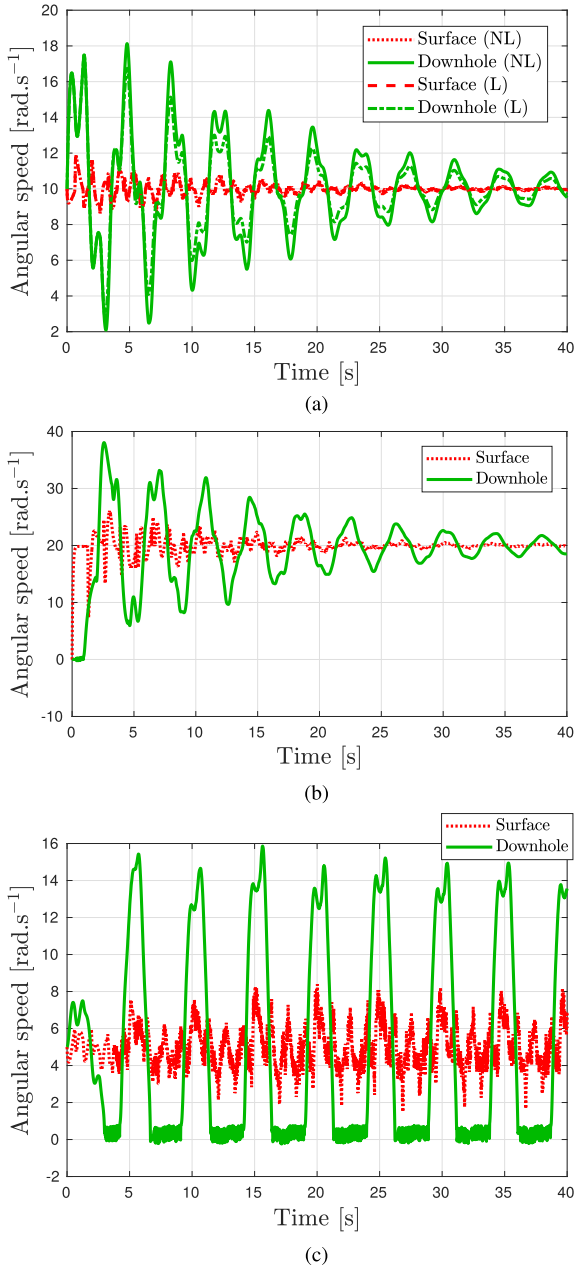

Fig. 7. Numerical simulations for systems (10) and (25) with $k_p = 10^{-3}$ and $k_i = 10$. (a) Systems (10) and (25)—$\Omega_0 = \phi^1 = 10$, $\phi^0(x) = (1 + 0.32\sin(x))\int_0^x \phi_x^\infty(s)ds$, and $Z(0) = (z_1^\infty\ z_2^\infty)^\top$. (b) System (25)—$\Omega_0 = 20$, $\phi^0 = 0$, $\phi^1 = 0$, and $Z(0) = 0_{2,1}$. (c) System (25)—$\Omega_0 = \phi^1 = 5$, $\phi^0(x) = (1 + 0.1\sin(x))\int_0^x \phi_x^\infty(s)ds$, and $Z(0) = (z_1^\infty\ z_2^\infty)^\top$.

The higher Ω_0 is, the larger the basin of attraction is. Indeed, the regulation tries to bring the system into the "quasi-linear" zone of T_{nl}, where it is close to a constant $T_{\min}$, as seen in Fig. 3, and consequently, the stick-slip phenomenon may occur at the beginning, but it is not effective for a long time as shown in Fig. 7(b) which is a numerical simulation on the nonlinear model with a zero initial condition.

The real challenge is then the case of low-desired angular velocities Ω_0. The result of a simulation on the nonlinear model for $\Omega_0 = 5$ rad.s^{-1} ($k_p = 10^{-3}$, $k_i = 10$) is shown in Fig. 7(c). First of all, note that the oscillations are with

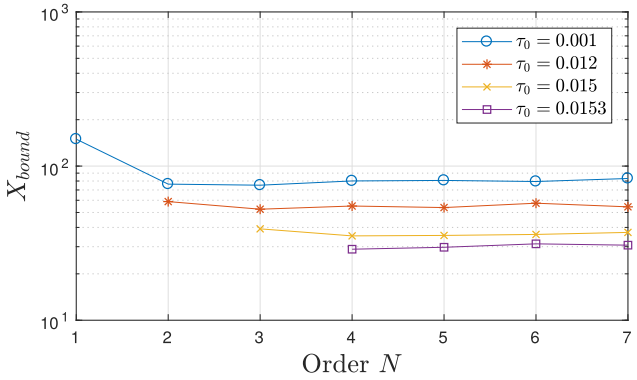

Fig. 8. Solution X_{bound} of BMI (27) for $k_p = 10^{-3}$, $k_i = 10$, and $\Omega_0 = 5$ and some values of τ_0. The limit is $X_{\text{bound}} = 28$.

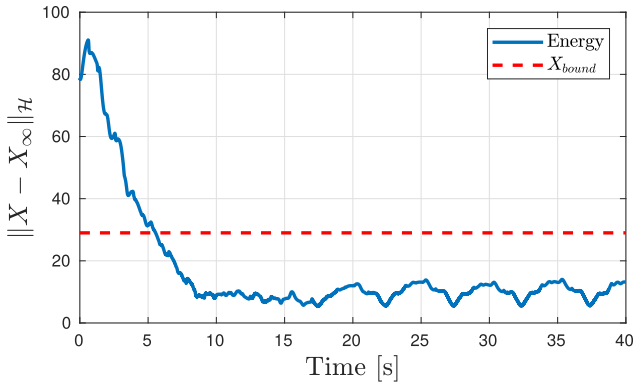

Fig. 9. Energy of X with the nonlinear system for $k_p = 10^{-3}$, $k_i = 10$, and $\Omega_0 = 5$. The initial condition is the same as in Fig. 5.

a frequency of 0.2 Hz and with an amplitude of roughly 15 rad.s^{-1}. This is very close to what has been estimated using Fig. 2. Then, the model presented in Section II seems to be a valid approximation of the real behavior, at least concerning the stick-slip phenomenon.

C. Practical Stability Analysis

Now, one can evaluate the amplitude of the oscillations using Theorem 2 with $k_p = 10^{-3}$ and $k_i = 10$. The result for several values of τ_0 and for an order between 0 and 7 is shown in Fig. 8. Note that after order 8, there are numerical errors in the optimization process, and the result is not accurate. The maximum τ_0 is $2\mu_{\max} = 0.0155$ and the higher τ_0 is, the better is the optimization. It appears that for $k_i = 10$, $k_p = 10^{-3}$, and $\Omega_0 = 5$, the optimal X_{bound} is around 28.

Fig. 9 shows the energy of the system as a function of time. One can see that the bound X_{bound} is quite accurate since the error between the maximum of the auto-oscillations and X_{bound} is around 53%. Moreover, note that $\max|z_1 - \Omega_0| = 11.7 = 0.4\ X_{\text{bound}}$, in other words, nearly half of the oscillations are concentrated in the variable z_1, which means the stick-slip mostly acts on the variable z_1 and does not affect much the rest of the system. In particular, it seems very difficult to estimate the variation of z_1 knowing only $\phi_t(0, t)$.

The final observation is about the variation of X_{bound} for different Ω_0. This is shown in Fig. 10. Up to errors in

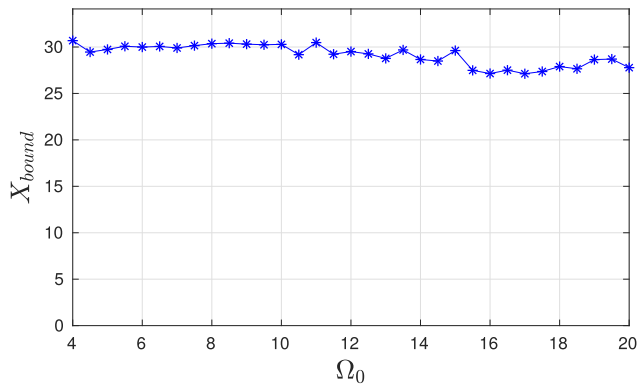

Fig. 10. Solution X_{bound} of BMI (27) for $k_p = 10^{-3}$, $k_i = 10$, $\tau_0 = 0.0153$, and $N = 5$.

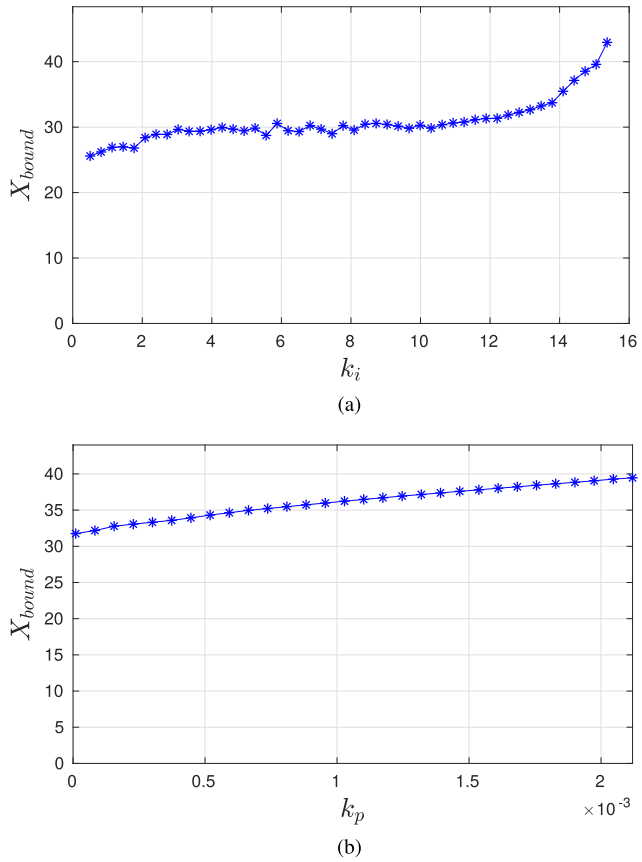

Fig. 11. Minimal X_{bound} obtained using Theorem 2 with $\Omega_0 = 5$ and $N = 5$. (a) X_{bound} for $k_p = 10^{-3}$ but with different values of k_i. (b) X_{bound} for $k_i = 10$ but with different values of k_p.

the numerical optimization, it seems that there is not an important variation of X_{bound} when Ω_0 increases. This is counter-intuitive and does not reflect the observations made with Fig. 7. One explanation is that we did not state that T_{nl} is a strictly decreasing function for positive θ.

D. Design of a PI Controller

Finally, the problem stated at the beginning of this article was to find the best PI controller, meaning that it minimizes X_{bound}. The plot in Fig. 11(a) shows that the value of the integral gain k_i does impact the oscillations due to stick-slip since X_{bound} increases from 25 to 43 for $k_i \in [0.5, 16]$, and the LMIs become infeasible after this point (these values have been obtained with $\Omega_0 = 5$, $k_p = 10^{-3}$, and $N = 5$).

To stay robustly stable against small delay in the loop, as noted in Section IV-C, we should consider $0 \leq k_p \leq 2.1 \cdot 10^{-3}$ which does not offer a large set of choices. For $k_i = 10$, we get Fig. 11(b). It appears that the minimum of X_{bound} is obtained for k_p close to 0. Consequently, increasing the gain k_p seems not to reduce the stick-slip effect. Consequently, even if a PI controller does not weaken the stick-slip effect, the equilibrium point of the controlled system is practically stable. Moreover, it does enable an oscillation around the desired equilibrium point and a local convergence to that point.

VII. Conclusion

This article focused on the analysis of the performance of a PI controller for a drilling pipe. First, a discussion between the existing models in the literature allows us to conclude that the infinite-dimensional model is closer to the real drilling pipe and should then be used for simulations and analysis. Based on this last model, the exponential stability of the closed-loop system was ensured using a Lyapunov functional depending on projections of the infinite-dimensional state on a polynomials basis. This approach enables getting exponential stability of the linear system with an estimation of the decay rate. This result was then extended to the nonlinear case considering practical stability. The example section shows that it is possible to get an estimate of the smallest attractive and invariant set and that this estimate is close to the minimal one. Further research would focus on similar analysis but using different controllers as the ones developed in [13], [30], [41], or [38, Ch. 10].

Appendix
Legendre Polynomials and Bessel Inequality

The performance of the Lyapunov functional (16) highly depends on the projection methodology developed in [42]. To help the reader to better understand the proof of Theorem 1, a definition and some properties of Legendre polynomials are reminded. More information can be found in [17].

Definition 4: The orthonormal family of Legendre polynomials $\{\mathcal{L}_k\}_{k\in\mathbb{N}}$ on $L^2([0,1])$ embedded with the canonical inner product is defined as follows:

$$\mathcal{L}_k(x) = (-1)^k \sum_{l=0}^{k} (-1)^l \binom{k}{l} \binom{k+l}{l} x^l$$

where $\binom{k}{l} = (k!/l!(k-l)!)$.

Their expended formulation is not useful in this article, but the two following lemmas are of main interest.

Lemma 4: For any function $\chi \in L^2$ and symmetric positive matrix $R \in \mathbb{S}_+^2$, the following Bessel-like integral inequality holds for all $N \in \mathbb{N}$:

$$\int_0^1 \chi^\top(x) R \chi(x) dx \geqslant \sum_{k=0}^{N} (2k+1) \mathfrak{X}_k^\top R \mathfrak{X}_k \qquad (31)$$

where $\mathfrak{X}_k$ is the projection coefficient of χ with respect to the Legendre polynomial $\mathcal{L}_k$ as defined in (15).

Lemma 5: For any function $\chi \in L^2$ satisfying (15), the following expression holds for any N in $\mathbb{N}$:

$$\begin{bmatrix} \dot{\mathfrak{X}}_0 \\ \vdots \\ \dot{\mathfrak{X}}_N \end{bmatrix} = \mathbb{1}_N \chi(1) - \bar{\mathbb{1}}_N \chi(0) - L_N \begin{bmatrix} \mathfrak{X}_0 \\ \vdots \\ \mathfrak{X}_N \end{bmatrix} \tag{32}$$

where $L_N, \mathbb{1}_N$ and $\bar{\mathbb{1}}_N$ are defined in (13).

Proof: This proof is highly inspired from [8]. Since $\chi \in L^2$ satisfies (15), (18) can be derived and the following holds:

$$\dot{\mathfrak{X}}_k = \Lambda[\chi(x)\mathcal{L}_k(x)]_0^1 - \Lambda \int_0^1 \chi(x)\mathcal{L}'(x)dx - \frac{\gamma_t}{2}\begin{bmatrix} 1 & 1 \\ 1 & 1 \end{bmatrix}\mathfrak{X}_k.$$

As noted in [17], the interesting properties of Legendre polynomials are stated as follows.

1) The boundary conditions on $\mathcal{L}_k$ ensures $\mathcal{L}_k(0) = (-1)^k$ and $\mathcal{L}_k(1) = 1$;
2) The derivation rule for Legendre polynomials is $(d/dx)\mathcal{L}_k(x) = \sum_{j=0}^{k} \ell_{j,k}\mathcal{L}_j(x)$.

These two properties lead to the proposed result in (32). ■

REFERENCES

[1] U. J. F. Aarsnes and O. M. Aamo, "Linear stability analysis of self-excited vibrations in drilling using an infinite dimensional model," *J. Sound Vib.*, vol. 360, pp. 239–259, Jan. 2016.

[2] U. J. F. Aarsnes and J. S. Roman, "Torsional vibrations with bit off bottom: Modeling, characterization and field data validation," *J. Petroleum Sci. Eng.*, vol. 163, pp. 712–721, Apr. 2018.

[3] B. Armstrong-Helouvry, "Stick-slip arising from stribeck friction," in *Proc. IEEE Int. Conf. Robot. Automat.*, May 1990, pp. 1377–1382.

[4] B. Armstrong-Hélouvry, P. Dupont, and C. C. De Wit, "A survey of models, analysis tools and compensation methods for the control of machines with friction," *Automatica*, vol. 30, pp. 1083–1138, Jul. 1994.

[5] M. Barreau, *Stability analysis of coupled ordinary differential systems with a string equation—Application to a Drilling Mechanism*. Toulouse, France: Université Fédérale Toulouse Midi-Pyrénées, 2019.

[6] M. Barreau, F. Gouaisbaut, A. Seuret, and R. Sipahi, "Input/output stability of a damped string equation coupled with ordinary differential system," *Int. J. Robust Nonlinear Control*, vol. 28, no. 18, pp. 6053–6069, Dec. 2018.

[7] M. Barreau, A. Seuret, and F. Gouaisbaut, "Exponential Lyapunov stability analysis of a drilling mechanism," in *Proc. 57st IEEE Conf. Decis. Control (CDC)*, Dec. 2018, pp. 6579–6584.

[8] M. Barreau, A. Seuret, F. Gouaisbaut, and L. Baudouin, "Lyapunov stability analysis of a string equation coupled with an ordinary differential system," *IEEE Trans. Autom. Control*, vol. 63, no. 11, pp. 3850–3857, Nov. 2018.

[9] G. Bastin and J.-M. Coron, *Stability and Boundary Stabilization of 1-D Hyperbolic Systems*, vol. 88. Basel, Switzerland: Birkhäuser, 2016.

[10] H. I. Basturk, "Observer-based boundary control design for the suppression of stick–slip oscillations in drilling systems with only surface measurements," *J. Dyn. Syst., Meas., Control*, vol. 139, no. 10, Oct. 2017, Art. no. 104501.

[11] A. Bisoffi, M. Da Lio, A. R. Teel, and L. Zaccarian, "Global asymptotic stability of a PID control system with Coulomb friction," *IEEE Trans. Autom. Control*, vol. 63, no. 8, pp. 2654–2661, Aug. 2017.

[12] D. Bresch-Pietri and M. Krstic, "Output-feedback adaptive control of a wave PDE with boundary anti-damping," *Automatica*, vol. 50, no. 6, pp. 1407–1415, 2014.

[13] C. Canudas-de-Wit, F. Rubio, and M. Corchero, "D-OSKIL: A new mechanism for controlling stick-slip oscillations in oil well drillstrings," *IEEE Trans. Control Syst. Technol.*, vol. 16, no. 6, pp. 1177–1191, Nov. 2008.

[14] N. Challamel, "Rock destruction effect on the stability of a drilling structure," *J. Sound Vibrat.*, vol. 233, no. 2, pp. 235–254, 2000.

[15] A. P. Christoforou and A. S. Yigit, "Fully coupled vibrations of actively controlled drillstrings," *J. Sound Vibrat.*, vol. 267, no. 5, pp. 1029–1045, 2003.

[16] J.-M. Coron, "Control and nonlinearity," in *Mathematical Surveys and Monographs*. Providence, RI, USA: AMS, 2007, no. 136.

[17] R. Courant and D. Hilbert, *Methods of Mathematical Physics*. Hoboken, NJ, USA: Wiley, 1989.

[18] Y. Ebihara, D. Peaucelle, and D. Arzelier, *S-Variable Approach to LMI-Based Robust Control, Communications and Control Engineering*, vol. 17. London, U.K.: Springer, 2015.

[19] A. F. Filippov, "Classical solutions of differential equations with multi-valued right-hand side," *SIAM J. Control*, vol. 5, no. 4, pp. 609–621, 1967.

[20] E. Fridman, S. Mondié, and B. Saldivar, "Bounds on the response of a drilling pipe model," *IMA J. Math. Control Inf.*, vol. 27, no. 4, pp. 513–526, 2010.

[21] J. K. Hale and S. M. V. Lunel, "Effects of small delays on stability and control," in *Operator Theory and Analysis*. Basel, Switzerland: Birkhäuser, 2001, pp. 275–301.

[22] A. J. Helmicki, C. A. Jacobson, and C. N. Nett, "Ill-posed distributed parameter systems: A control viewpoint," *IEEE Trans. Autom. Control*, vol. 36, no. 9, pp. 1053–1057, Sep. 1991.

[23] D. Karnopp, "Computer simulation of stick-slip friction in mechanical dynamic systems," *J. Dyn. Syst., Meas., Control*, vol. 107, no. 1, pp. 100–103, Mar. 1985.

[24] H. K. Khalil, *Nonlinear Systems*. London, U.K.: Pearson Education, 1996.

[25] M. Krstic, *Delay Compensation for Nonlinear, Adaptive, and PDE Systems*. Cambridge, MA, USA: Birkhäuser, 2009.

[26] N. Levinson, "Transformation theory of non-linear differential equations of the second order," *Ann. Math.*, vol. 45, no. 4, pp. 723–737, 1944.

[27] X. Liu, N. Vlajic, X. Long, G. Meng, and B. Balachandran, "Coupled axial-torsional dynamics in rotary drilling with state-dependent delay: Stability and control," *Nonlinear Dyn.*, vol. 78, no. 3, pp. 1891–1906, Nov. 2014.

[28] J. Löfberg, "YALMIP: A toolbox for modeling and optimization in MATLAB," in *Proc. IEEE Int. Conf. Robot. Automat.*, Sep. 2004, pp. 284–289.

[29] O. Morgul, "On the stabilization and stability robustness against small delays of some damped wave equations," *IEEE Trans. Autom. Control*, vol. 40, no. 9, pp. 1626–1630, Sep. 1995.

[30] E. Navarro-López, "An alternative characterization of bit-sticking phenomena in a multi-degree-of-freedom controlled drillstring," *Nonlinear Anal., Real World Appl.*, vol. 10, no. 5, pp. 3162–3174, 2009.

[31] E. Navarro-López and D. A. Cortes, "Sliding-mode control of a multi-DOF oilwell drillstring with stick-slip oscillations," in *Proc. Amer. Control Conf.*, Jul. 2007, pp. 3837–3842.

[32] E. Navarro-López and R. Suarez, "Practical approach to modelling and controlling stick-slip oscillations in oilwell drillstrings," in *Proc. IEEE Int. Conf. Control Appl.*, vol. 2, Sep. 2004, pp. 1454–1460.

[33] C. Prieur, S. Tarbouriech, and J. M. G. da Silva, "Wave equation with cone-bounded control laws," *IEEE Trans. Autom. Control*, vol. 61, no. 11, pp. 3452–3463, Nov. 2016.

[34] T. Richard, C. Germay, and E. Detournay, "A simplified model to explore the root cause of stick–slip vibrations in drilling systems with drag bits," *J. Sound Vib.*, vol. 305, no. 3, pp. 432–456, 2007.

[35] C. Roman, D. Bresch-Pietri, E. Cerpa, C. Prieur, and O. Sename, "Backstepping observer based-control for an anti-damped boundary wave PDE in presence of in-domain viscous damping," in *Proc. IEEE 55th Conf. Decis. Control (CDC)*, Dec. 2016, pp. 549–554.

[36] M. Safi, L. Baudouin, and A. Seuret, "Tractable sufficient stability conditions for a system coupling linear transport and differential equations," *Syst. Control Lett.*, vol. 110, pp. 1–8, Dec. 2017.

[37] C. Sagert, F. Di Meglio, M. Krstic, and P. Rouchon, "Backstepping and flatness approaches for stabilization of the stick-slip phenomenon for drilling," *IFAC Proc. Volumes*, vol. 46, no. 2, pp. 779–784, 2013.

[38] B. Saldivar, I. Boussaada, H. Mounier, and S.-I. Niculescu, *Analysis and Control of Oilwell Drilling Vibrations: A Time-Delay Systems Approach*. Cham, Switzerland: Springer, 2015.

[39] B. Saldivar, S. Mondié, and J. C. Ávila Vilchis, "The control of drilling vibrations: A coupled PDE-ODE modeling approach," *Int. J. Appl. Math. Comput. Sci.*, vol. 26, no. 2, pp. 335–349, 2016.

[40] B. Saldivar, S. Mondié, S.-I. Niculescu, H. Mounier, and I. Boussaada, "A control oriented guided tour in oilwell drilling vibration modeling," *Annu. Rev. Control*, vol. 42, pp. 100–113, Sep. 2016.

[41] A. Sevrarens, M. J. G. Molengraft, J. J. Kok, and L. van den Steen, "H∞ control for suppressing stick-slip in oil well drillstring," *IEEE Trans. Control Syst.*, vol. 18, no. 4, pp. 19–30, May 1998.
[42] A. Seuret and F. Gouaisbaut, "Hierarchy of LMI conditions for the stability analysis of time-delay systems," *Syst. Control Lett.*, vol. 81, pp. 1–7, Jal. 2015.
[43] S. Tarbouriech, G. Garcia, J. M. G. da Silva, Jr, and I. Queinnec, *Stability and Stabilization of Linear Systems with Saturating Actuators*. London, U.K.: Springer-Verlag, 2011.
[44] A. Terrand-Jeanne, V. Andrieu, M. Tayakout-Fayolle, and V. Dos Santos Martins, "Regulation of inhomogeneous drilling model with a P-I controller," *IEEE Trans. Autom. Control*, to be published.
[45] A. Terrand-Jeanne, V. Dos Santo Martins, and V. Andrieu, "Regulation of the downside angular velocity of a drilling string with a P-I controller," in *Proc. Eur. Control Conf. (ECC)*, Jun. 2018, pp. 2647–2652.
[46] K.-C. Toh, M. J. Todd, and R. H. Tütüncü, "SDPT3—A MATLAB software package for semidefinite programming," *Optim. Methods Softw.*, vol. 11, nos. 1–4, pp. 545–581, 1999.
[47] W. R. Tucker and C. Wang, "On the effective control of torsional vibrations in drilling systems," *J. Sound Vibrat.*, vol. 224, no. 1, pp. 101–122, 1999.
[48] M. Tucsnak and G. Weiss, *Observation and Control for Operator Semigroups*. Basel, Switzerland: Birkhäuser, 2009.
[49] W., Jr., Weaver, S. P. Timoshenko, and D. H. Young, *Vibration Problems in Engineering*. Hoboken, NJ, USA: Wiley, 1990.

Matthieu Barreau received the Engineering Degree in aeronautical engineering from the Institut Supérieur de l'Aéronautique et de l'Espace, Toulouse, France, in 2016, the Diplôme d'Ingénieur and Civilingenjörsexamen degree in space engineering, with specialization in system engineering, from the KTH Royal Institute of Technology, Stockholm, Sweden, in 2015, in 2016, the Ph.D. degree from the Laboratory for Analysis and Architecture of Systems, Centre national de la recherche scientifique, Toulouse, and the Diplôme de Doctorate degree in system theory from Paul Sabatier University, Toulouse, in 2019.

His Ph.D. study was carried out under the supervision of A. Seuret and F. Gouaisbaut. His current research interests include stability analysis of infinite-dimensional systems with a particular focus on drilling systems.

Frédéric Gouaisbaut was born in Rennes, France, in April 1973. He received the Dipl.-Ing. degree (Engineer) in automatic control from the Ecole Centrale de Lille, Villeneuve-d'Ascq, France, in September 1997, and the D.E.A. degree (master) in automatic control from Lille 1 University, Villeneuve-d'Ascq, in September 1997, and the Ph.D. degrees from the Laboratoire d'Automatique, Génie Informatique et Signal (LAGIS), Ecole Centrale de Lille, Lille, France, and Lille 1 University, in October 2001.

Since October 2003, he has been an Associate Professor with Paul Sabatier University, Toulouse, France. His current research interests include time-delay systems, quantized systems, and robust control.

Alexandre Seuret was born in France in 1980. He received the Engineering Degree from the Ecole Centrale de Lille, Lille, France, the master's degree in system theory from Lille 1 University, Villeneuve-d'Ascq, France, in 2003, and the Ph.D. degree in automatic control from the Ecole Centrale de Lille and Lille 1 University in 2006.

From 2006 to 2008, he held 1-year postdoctoral positions with the University of Leicester, Leicester, U.K., and the KTH Royal Institute of Technology, Stockholm, Sweden. From 2008 to 2012, he was a Junior CNRS Researcher (Chargé de Recherche) with the Grenoble Images Parole Signal Automatique Laboratory, Grenoble, France. Since 2012, he has been a Junior CNRS Researcher with the Laboratory for Analysis and Architecture of Systems, Toulouse, France. His current research interests include time-delay systems, networked control systems, and multiagent systems.